PHLPP1 Counter-regulates STAT1-mediated Inflammatory Signaling

Ksenya Cohen-Katsenelson[1,5], Joshua D. Stender[2,5], Agnieszka T. Kawashima[1,5], Gema Lordén[1], Satoshi Uchiyama[3], Victor Nizet[3,4], Christopher K. Glass[2], and Alexandra C. Newton*[1]

[1]Department of Pharmacology

[2]Department of Cellular and Molecular Medicine

[3]Department of Pediatrics

[4]Skaggs School of Pharmacy and Pharmaceutical Sciences,

[5]Biomedical Sciences Graduate Program, University of California at San Diego, CA 92093

[5]These authors contributed equally

*Correspondence to: Alexandra C. Newton

Tel.: 858-534-4527; Fax: 858-822-5888

anewton@ucsd.edu

Running title: PHLPP1 Suppresses STAT1-mediated Inflammatory Signaling

ABSTRACT

Inflammation is an essential aspect of innate immunity but also contributes to diverse human diseases. Although much is known about the kinases that control inflammatory signaling, less is known about the opposing phosphatases. Here we report that deletion of the gene encoding PH domain Leucine-rich repeat Protein Phosphatase 1 (PHLPP1) protects mice from lethal lipopolysaccharide (LPS) challenge and live *Escherichia coli* infection. Investigation of PHLPP1 function in macrophages reveals that it controls the magnitude and duration of inflammatory signaling by dephosphorylating the transcription factor STAT1 on Ser727 to inhibit its activity, reduce its promoter residency, and reduce the expression of target genes involved in innate immunity and cytokine signaling. This previously undescribed function of PHLPP1 depends on a bipartite nuclear localization signal in its unique N-terminal extension. Our data support a model in which nuclear PHLPP1 dephosphorylates STAT1 to control the magnitude and duration of inflammatory signaling in macrophages.

HIGHLIGHTS

- PHLPP1 controls the transcription of genes involved in inflammatory signaling
- PHLPP1 dephosphorylates STAT1 on Ser727 to reduce its transcriptional activity
- PHLPP1 has a nuclear localization signal and a nuclear exclusion signal
- Loss of PHLPP1 protects mice from sepsis-induced death

INTRODUCTION

Gene expression is an exquisitely regulated process that maintains cellular homeostasis and orchestrates appropriate responses to environmental stimuli such as hormones, cytokines, and pathogenic microbes (Dawson and Kouzarides, 2012; Flavahan et al., 2017). Homeostatic control of inflammatory genes is particularly relevant to cancer since chronic inflammation promotes tumorigenesis and influences patient response to cancer therapeutics (Coussens and Werb, 2002; Grivennikov et al., 2010). Dysregulated gene expression, a hallmark of cancer, can arise from mutations in transcription factors (exemplified by p53 (Sabapathy and Lane, 2018)), alterations in signaling pathways controlling transcription factor function (for example, hormone-dependent transcription factors in prostate and breast cancers (Jernberg et al., 2017; Pejerrey et al., 2018)), or upregulation of oncogenic transcription factors (notably c-myc, which regulates essential cell-cycle checkpoints (Kalkat et al., 2017)). Aberrant protein phosphorylation underpins all of these mechanisms, via dysregulation of signaling pathways, alterations in transcription factor machinery, and/or effects on the chromatin epigenetic landscape (Rossetto et al., 2012; Whitmarsh and Davis, 2000). Thus, targeting phosphorylation mechanisms is of considerable therapeutic interest.

Macrophages are among the first responders to infection, engaging foreign pathogens via pattern recognition receptors, including the Toll-like receptors (TLRs). TLRs are a conserved family of cell surface or phagosome-associated receptors that discriminate distinct features of microbial and viral pathogens, including lipoproteins (TLR1/2/6), lipopolysaccharide (LPS) (TLR4), flagellin (TLR5), single-stranded RNA (TLR7/8), double-stranded RNA (TLR3), and double-stranded DNA (TLR9) (Karin et al., 2006; O'Neill et al., 2013). Upon pathogen recognition by TLRs, a pro-inflammatory response is initiated that activates the signal-dependent

transcription factors nuclear factor-κ B (NFκB), activator protein 1 (AP1), interferon response factors (IRFs), and, through secondary mechanisms, the signal transducer and activator of transcription (STAT) protein family (O'Neill et al., 2013). These activated transcription factors function in a combinatorial manner to drive expression of antimicrobial and inflammatory response genes that aid in elimination of foreign pathogens. However, while inflammation is required for protection against foreign microbes, it can lead to excessive cytokine production, chronic inflammation, and cancer if not properly resolved (Coussens and Werb, 2002; Fullerton and Gilroy, 2016; Grivennikov et al., 2010). Thus, macrophages have evolved regulatory mechanisms to resolve inflammatory responses in a timely manner, including shut down of STAT1 signaling pathways by the suppressor of cytokine signaling (SOCS) family of proteins (O'Shea and Murray, 2008), suppression of nitric oxide production by the enzyme arginase (Wynn and Vannella, 2016), and inhibition of a key subset of NFκB-dependent genes by anti-inflammatory omega-3 fatty acids, (Oishi et al., 2017).

STAT1 is the founding member of the STAT transcription factor family and serves as a paradigm for how phosphorylation regulates transcription factor structure, function, and localization (Darnell et al., 1994; Stark and Darnell, 2012). In the canonical pathway, STATs are recruited from the cytosol to cytokine-bound and Tyr-phosphorylated receptors where they are phosphorylated on a key Tyr residue (Tyr701 for STAT1) by Janus Kinases (JAKs). This phosphorylation event promotes STAT dimerization and nuclear entry, allowing STAT binding to specific promoter sequences and thus initiating gene transcription. Upon promoter binding, STATs become additionally phosphorylated on a regulatory Ser residue at a MAPK consensus sequence (Ser727 for STAT1), a modification that enhances their transcriptional activity (Darnell, 1997; Sadzak et al., 2008; Wen et al., 1995b; Whitmarsh and Davis, 2000).

Importantly, STAT1 transduces signals from type I and II interferons (IFNs), resulting in binding to IFN-stimulated response elements (ISREs) and to IFN-gamma (IFNγ)-activated site (GAS) elements in the promoters of IFN-stimulated genes (ISGs), inducing their transcription and stimulating inflammation (Platanias, 2005). While the kinases that phosphorylate Tyr701 and Ser727 on STAT1 have been extensively studied, as have been the phosphatases that dephosphorylate Tyr701, the phosphatases that oppose the Ser727 phosphorylation are unknown.

PH domain Leucine-rich Repeat Protein Phosphatase 1 (PHLPP1) is one of the newest members of the phosphatome (Chen et al., 2017; Gao et al., 2005). Originally discovered for its function in suppressing growth factor signaling by dephosphorylating Akt on the hydrophobic motif site, Ser473 (Gao et al., 2005), the repertoire of PHLPP1 substrates is continually expanding (Grzechnik and Newton, 2016). PHLPP1 is a bona fide tumor suppressor: its expression is frequently lost in cancer and its genetic ablation in a mouse model results in prostate neoplasia (Chen et al., 2011; Liu et al., 2009). PHLPP1 is also involved in the immune response, where its dephosphorylation of Akt reduces the capacity of regulatory T cells to transduce T cell receptor signals, a key function in T cell development (Patterson et al., 2011). Recently, PHLPP1 was shown to suppress receptor tyrosine kinase gene expression and influence growth factor signaling, including that mediated by the epidermal growth factor (EGF) receptor (Reyes et al., 2014).

PHLPP1 is unusual among protein phosphatases in that its regulatory modules and catalytic domain are on the same polypeptide. Most notably, it has a PH domain essential for dephosphorylation of protein kinase C (PKC) (Gao et al., 2008), a PDZ ligand necessary for Akt recognition (Gao et al., 2005), and a leucine-rich repeat (LRR) segment required for transcriptional regulation of receptor tyrosine kinases (Reyes et al., 2014). In addition, PHLPP1

possesses an approximately 50 kDa N-terminal extension (NTE) of unknown function. Stoichiometric association with substrates by direct binding to the protein-interaction domains on PHLPP or common scaffolds (e.g. PDZ domain proteins such as Scribble (Li et al., 2011)) allows fidelity and specificity in PHLPP function, and may account for its >10-fold lower catalytic rate compared to the closely related phosphatase PP2Cα (Sierecki and Newton, 2014). Given its transcriptional regulation of at least one family of genes, PHLPP1 is an attractive pharmacological target for modulation of gene expression.

Here we report that nuclear-localized PHLPP1 opposes STAT1 Ser727 phosphorylation to inhibit its transcriptional activity and promote normal resolution of inflammatory signaling. We find that *Phlpp1*$^{-/-}$ mice have improved survival following infection with *Escherichia coli* (*E. coli*), indicating a role of the phosphatase in innate immunity. Since macrophages are key in the initial response to lipopolysaccharide (LPS) from Gram-negative bacteria such as *E. coli*, we further explored the role of PHLPP1 in controlling LPS-dependent signaling in this cell type. The STAT1 binding motif was identified from the most common promoter sequences of 199 genes that remained elevated following LPS treatment of bone marrow-derived macrophages (BMDMs) from *Phlpp1*$^{-/-}$ mice compared to those from wild-type (WT) mice. We validated common transcriptional targets of PHLPP1 and STAT1, showing that loss of PHLPP1 upregulated the transcription of several genes including guanylate binding protein 5 (*Gbp5*), whereas loss of STAT1 downregulated them. Dephosphorylation of STAT1 on Ser727 suppressed its transcriptional activity, and the cellular effects of PHLPP1 depend both on its catalytic activity and a previously undescribed nuclear localization signal (NLS). Taken together, our results identify PHLPP1 as a major player in the resolution of inflammatory signaling.

RESULTS

PHLPP1 regulates the innate immune response

To explore the role of PHLPP1 in acute inflammation, we examined the kinetics and outcome of sepsis-induced death caused by intraperitoneal (i.p.) injection of Gram-negative *E. coli* bacteria in WT and *Phlpp1*$^{-/-}$ mice. Surprisingly, absence of PHLPP1 provided a strong protective effect; at a dose where more than 50% of WT mice died within 12 h of *E. coli* challenge, 50% of the *Phlpp1*$^{-/-}$ mice remained alive after 10 days (**Figure 1A**). Similarly, *Phlpp1*$^{-/-}$ mice were protected from toxicity induced by the purified Gram-negative bacterial cell wall component LPS, with nearly half of the *Phlpp1*$^{-/-}$ mice alive after 10 days compared to only 1 out of 16 of the WT mice (**Figure 1B**). To understand the lower mortality rates in *Phlpp1*$^{-/-}$ mice, we measured levels of different cytokines in the serum of mice across a time course following LPS injection (**Figure 1C-E**). Serum levels of pro-inflammatory cytokine interleukin 6 (IL-6) were significantly increased in WT mice within 5 h of LPS injection, returning to baseline within 12 h (**Figure 1C**). In contrast, the *Phlpp1*$^{-/-}$ mice had 2-fold lower IL-6 levels at 5 h post-infection, but these levels were sustained for up to 24 h, suggestive of improper resolution of inflammation. Levels of another pro-inflammatory cytokine, IL-1β, were likewise consistently higher in *Phlpp1*$^{-/-}$ mice compared with WT mice (**Figure 1D**). By contrast, levels of anti-inflammatory cytokine IL-10 did not differ significantly between the WT and *Phlpp1*$^{-/-}$ mice (**Figure 1E**). These findings indicate an essential role for PHLPP1 in regulation of the innate immune response at the whole organism level.

Loss of PHLPP1 results in a increased STAT1-dependent transcription in macrophages

Since macrophages are a key cell type involved in the initial response to *E. coli* infection and LPS challenge, we analyzed the transcriptome of BMDMs isolated from WT or *Phlpp1*$^{-/-}$ mice before and after stimulation by the major LPS component, Kdo2-Lipid A (KLA), for 1, 6, or 24 h (**Figure 2A**). RNA-Seq analysis identified 1,654 mRNA transcripts induced more than two-fold by KLA treatment, with a false discovery rate (FDR) less than 0.05 at any of the time points. Expression of approximately 12% of these genes (199 genes; **Table S1**) was increased in macrophages from *Phlpp1*$^{-/-}$ mice compared to those from littermate control WT mice 6 h following KLA treatment; transcript levels of these genes remained significantly elevated (>two-fold) 24 h later. Another set of genes exhibited reduced expression 24 h following KLA treatment (144 genes; **Table S2**). Gene ontology analysis revealed that many of the genes whose expression was elevated in the *Phlpp1*$^{-/-}$ macrophages are associated with inflammatory signaling: these included genes annotated for their involvement in the innate immune response, cytokine-cytokine receptor interactions, LPS signaling, interferon-β response, and tumor necrosis factor (TNF) signaling-dependent pathways (**Figure 2B**). Genes significantly decreased in *Phlpp1*$^{-/-}$ compared to WT macrophages were enriched most significantly in nodes related to central carbon metabolism, and to a lesser extent, chronic inflammatory responses and LPS signaling (**Figure 2B**).

To gain insight into gene regulatory mechanisms affected by loss of PHLPP1, we performed *de novo* motif analysis of the promoters of upregulated genes in *Phlpp1*$^{-/-}$ macrophages using Hypergeometric Optimization of Motif EnRichment (HOMER), a suite of tools for motif discovery and Next Generation Sequencing (NGS) analysis (Heinz et al., 2010). This algorithm defines motifs that are statistically enriched in a targeted promoter list compared

to random promoter sequences with comparable GC content. The analysis revealed significant enrichment of STAT ($p<10^{-18}$) and IRF ($p<10^{-9}$) motifs (**Figure 2C**) in the promoters of genes whose expression was statistically increased in *Phlpp1*$^{-/-}$ macrophages compared to WT macrophages. Of the 199 genes with elevated expression, 46% of the genes had promoters with a consensus STAT binding motif, 51% had promoters with a potential binding site for IRF family of transcription factors, and 26% had promoters with predicted binding sites for both STAT and IRF (**Figure 2D**). We selected for further analysis three genes whose expression was elevated in the *Phlpp1*$^{-/-}$ compared to WT macrophages and which had proximal STAT1 binding motifs in their promoters: *Cd69*, *Ifit2*, and *Gbp5*. Normalized mRNA-Seq data for each of these three genes confirmed elevated mRNA levels in *Phlpp1*$^{-/-}$ macrophages compared to WT macrophages (**Figure 2E-G**). Thus, loss of PHLPP1 leads to sustained KLA-induced expression of genes involved in inflammation, of which 46% have predicted STAT motifs in their proximal regulatory regions.

If PHLPP1 suppresses STAT-regulated gene transcription, we reasoned that 1] knockdown of a STAT family member should reduce transcription of the same genes affected by loss of PHLPP1 and 2] knockdown of PHLPP1 should enhance STAT binding to its promoters. STAT1 is required for LPS-induced gene expression in macrophages (Ohmori and Hamilton, 2001) and implicated as a PHLPP1 target in iNOS regulation (Alamuru et al., 2014). STAT1 knockdown by siRNA in thioglycollate-elicited peritoneal macrophages resulted in a 2-fold reduction in KLA-induced transcription of *Cd69*, *Ifit2*, and *Gbp5* at 6 h compared to a control siRNA transfection, with transcript levels dropping to near baseline by 24 h (**Figure 3A-C**). The effect of PHLPP1 knockdown on STAT1 promoter occupancy was examined by chromatin immunoprecipitation (ChIP) using STAT1-specific antibodies. KLA induced STAT1 binding to

the promoters of *Cd69*, *Ifit2*, and *Gbp5*, with maximal binding observed 1 h post stimulation, followed by a decay in binding to near baseline after 24 h (**Figure 3D-F**). In contrast, binding to these promoters was enhanced and sustained in *Phlpp1*$^{-/-}$ macrophages relative to WT cells. The degree of enhancement and the kinetics of activation/resolution varied depending on the gene examined: PHLPP1 loss had the most robust early effect (1 h) on the *Ifit2* promoter and at a later time (24 h) on the *Cd69* promoter. Thus, PHLPP1 suppresses KLA-stimulated binding of STAT1 to its promoters and thereby reduces transcription of its target genes.

PHLPP1 binds to STAT1 and dephosphorylates Ser727

We next examined whether PHLPP1 affects the phosphorylation state of the two regulatory STAT1 phosphorylation sites, Ser727 and Tyr701. Primary BMDMs were isolated from WT and *Phlpp* $^{-/-}$ mice and the kinetics and magnitude of KLA-triggered phosphorylation at each of the two STAT1 sites were compared. Loss of PHLPP1 in BMDMs led to a robust increase in STAT1 phosphorylation on the regulatory site Ser727 but did not affect Tyr701 phosphorylation (**Figure 4A-B**). PHLPP1 loss also resulted in an increase in Erk phosphorylation at its activation loop sites, as previously reported (Reyes et al., 2014). Incubation of *in vitro* phosphorylated STAT1 with immunoprecipitated FLAG-tagged PHLPP1 resulted in dephosphorylation at Ser727, suggesting that PHLPP1 directly dephosphorylates STAT1 (**Figure 4C**). Furthermore, overexpression of PHLPP1 in HEK-293T cells reduced IFNγ-dependent phosphorylation of STAT1 on Ser727 but not on Tyr701 (**Figure 4D-E**). Thus, PHLPP1 selectively dephosphorylates the Ser727 regulatory phosphorylation on STAT1 in cells and *in vitro*.

Because the abundance of PHLPP1 in the cell is much lower than other phosphatases such as PP2A (Hein et al., 2015), we next sought to determine whether regulation of STAT1 promoter activity was solely due to PHLPP1 phosphatase activity or occurred in combination with other phosphatases. Taking advantage of the insensitivity of PHLPP phosphatases to the PP1/PP2A inhibitor okadaic acid (OA) (Gao et al., 2005), we examined whether OA treatment affected KLA-dependent changes on Ser727 phosphorylation in primary BMDMs from WT mice. **Figure 5A-B** shows that the KLA-induced increase in Ser727 phosphorylation was relatively insensitive to OA, under conditions where the phosphorylation of Erk (at Thr202/Tyr204) and Akt (at Thr308) was significantly increased upon OA addition. These data are consistent with PHLPP1, a PP2C family member, being the primary regulator of phosphorylation on the activity-tuning Ser727 site of STAT1.

We next addressed whether enhanced promoter binding of STAT1 upon loss of PHLPP1 resulted in enhanced transcriptional activation using a luciferase reporter assay. WT or *Phlpp1*$^{-/-}$ mouse embryonic fibroblasts (MEFs) were co-transfected with a firefly luciferase reporter construct containing GAS promoter elements, as well as a renilla luciferase controlled by a constitutive CMV promoter as an internal control. STAT1 promoter activity was assessed by monitoring luminescence following IFNγ stimulation. **Figure 6A** shows that STAT1 promoter activity was significantly higher in *Phlpp1*$^{-/-}$ MEFs compared to WT MEFs at both 6 h and 24 h. Pre-treatment of cells with okadaic acid, under conditions that increased the phosphorylation of PP2A-sensitive substrates (see **Figure 5A**), had no effect on STAT1 promoter activity (**Figure 6A**). Because STAT1 functions in the nucleus, we next asked whether PHLPP1 regulation of STAT1 occurs in the cytoplasm or nucleus. To this end, we assessed the effect of expressing either the PP2C domain of PHLPP1 or a nuclear-targeted (NLS) PP2C domain of PHLPP1 on

IFNγ-induced STAT1 promoter activity via the GAS luciferase assay (**Figure 6B**). The overexpressed PP2C domain of PHLPP1 (**Figure 6C, blue**) was considerably less effective in inhibiting STAT1 promoter activity compared to full-length PHLPP1 (**Figure 6B, red**). However, forcing the PP2C domain into the nucleus by attaching an NLS to its N-terminus inhibited STAT1 promoter activity as effectively as overexpression of full-length PHLPP1 (**Figure 6B, orange**). Analysis of the subcellular localization of the constructs used in this experiment revealed that full-length PHLPP1 was primarily cytosolic, the isolated PP2C domain had increased nuclear localization, and the NLS-PP2C was enriched in the nucleus (**Figure S2**). To address whether PHLPP1 catalytic activity is required for STAT1 regulation, we utilized a phosphatase-dead PP2C domain in which two active site residues, Asp1210 and Asp1413 (Sierecki and Newton, 2014) were mutated to Ala (DDAA). The catalytically-inactive NLS-PP2C was no longer able to suppress STAT1 activity (**Figure 6C, purple**); immunohistochemistry confirmed its nuclear localization (**Figure S1**). Thus, both the catalytic activity and nuclear localization of PHLPP1 are necessary for it to regulate STAT1 transcriptional activity.

PHLPP1 has a bipartite Nuclear Localization Signal in its N-Terminal Extension

Bioinformatics analysis of the sequence of PHLPP1 using SeqNLS (Lin and Hu, 2013) revealed a potential Arg-rich bipartite NLS (^{92}RRRRR-X-^{122}RRGRLKR) in the N-terminal extension unique to the PHLPP1 isozyme (**Figure 6D**). To test whether these basic segments function as an NLS, we examined the subcellular localization in HeLa cells of the NTE alone or NTE in which the basic residues in each or both halves of the potential bipartite NLS were mutated to Ala (**Figure 6E**). Immunocytochemistry revealed that the NTE localizes to the

nucleus. Mutation of the first NLS or the second NLS increased the distribution of the NTE to the cytosol, and mutation of both decreased the nuclear:cytoplasmic ratio to be comparable to that of a construct of the NTE with a strong Nuclear Exclusion Signal (NES) (LALKLAGLDI from PKI (Wen et al., 1995a) (**Figure 6F**). Full-length PHLPP1 was primarily cytosolic, leading us to ask whether there may also be an NES. Bioinformatics analysis of the primary sequence identified a potential Leu-rich NES (Fu et al., 2011) immediately following the last LRR and preceding the phosphatase domain (**Figure S3**). Attachment of this 14-residue sequence to the N-terminus of the NTE resulted in distribution of the NTE to the cytosol (**Figure S3**). Thus, PHLPP1 nuclear localization is controlled by a bipartite NLS in the NTE and is opposed by an NES following the LRR. Lastly, we examined the effect of mutating the NLS on the ability of full-length PHLPP1 to reduce STAT1 transcriptional activity as assessed using the GAS promoter assay. The reduction in IFNγ-induced STAT1 activity resulting from PHLPP1 overexpression (**Figure 6G**, red) was abolished upon mutation of NLS2 (**Figure 6G**, brown) or both halves of the NLS (NLS1/2) (**Figure 6G**, purple). Mutation of NLS1 had an intermediate effect (**Figure 6G**, blue). These data reveal that a bipartite NLS in the NTE of PHLPP1 localizes PHLPP1 to the nucleus, where it suppresses the transcriptional activity of STAT1.

We next assessed which domain of PHLPP1 contributes to the observed regulation of STAT1 activity on the GAS promoter. Overexpression of full-length PHLPP1 in HEK-293T cells markedly reduced GAS promoter activity (**Figure 7A, red**) compared to the vector only control (**Figure 7A, black**). A construct of PHLPP1 lacking the NTE (deletion of first 512 amino acids of its N-terminus; P1ΔNTE, blue) was less effective than full-length PHLPP1 in reducing STAT1 activity, whereas a construct comprised of just the NTE (amino acids 1-512, green) caused a significant increase in GAS promoter activity, suggesting a dominant-negative function

of this segment. Co-immunoprecipitation assays revealed a robust interaction of STAT1 with the immunoprecipitated NTE of PHLPP1, in contrast to barely detectable binding of STAT1 to PHLPP1 lacking the NTE (**Figure 7B**). Intermediate binding was observed between STAT1 and full-length PHLPP1. Quantification of three independent experiments revealed that the isolated NTE of PHLPP1 binds STAT1 approximately five times more strongly than full-length PHLPP1 and 26 times more strongly than PHLPP1 lacking the NTE (**Figure 7C**). These data reveal that the NTE of PHLPP1 interacts with STAT1 and reduces its promoter activity.

DISCUSSION

The finding that *Phlpp1*$^{-/-}$ mice are protected from LPS-induced death allowed us to identify PHLPP1 as a physiologically relevant phosphatase in the overall innate immune response. It is likely that this immunoregulatory phenotype reflects roles of PHLPP1 in several immune cell types, and future studies of mice with cell-specific deletions of *Phlpp1* will be of great interest. Investigation of *Phlpp1*$^{-/-}$ macrophages indicates a significant role in counter-regulation of STAT1-dependent transcription that emerges as a secondary response to TLR4 ligation. Our mechanistic analyses show that PHLPP1 dephosphorylates STAT1 on a key regulatory site to suppress its transcriptional activity towards an array of genes involved in mounting an inflammatory response to IFNγ. Specifically, PHLPP1 directly dephosphorylates Ser727 on STAT1 *in vitro* and specifically suppresses phosphorylation of Ser727, but not Tyr701, on STAT1 in cells, correlating to decreased transcriptional activity of STAT1 at one of its major binding sites, the GAS promoter. The intrinsic catalytic activity and nuclear localization of PHLPP1 is required for this transcriptional regulation; while the isolated PP2C domain is not efficient in suppressing GAS promoter activity, forcing the PP2C domain into the nucleus is as effective as the full-length phosphatase in controlling transcriptional activity. Nuclear localization of the full-length enzyme is driven by a bipartite NLS we identify in the NTE. Elimination of PHLPP1 results in global changes in LPS-dependent transcriptional regulation, with 20% of the approximately 2,000 genes whose expression changes upon LPS stimulation differing by more than two-fold in BMDMs from *Phlpp1*$^{-/-}$ mice compared to WT mice.

Phosphorylation of STAT1 on Ser727 has been proposed to occur following the binding of the Tyr-phosphorylated STAT1 dimer to chromatin (Sadzak et al., 2008). Ser727 phosphorylation on the C-terminal transactivation domain of STAT1 is necessary for maximal

transcriptional activity. Identification of PHLPP1 as a phosphatase that opposes this phosphorylation provides a mechanism to counter-regulate the activity of this key transcription factor. Several lines of evidence suggest that PHLPP1 may be the major phosphatase that controls this regulatory site. First, genetic depletion of PHLPP1 increases both STAT1 Ser727 phosphorylation and transcriptional activity at the GAS promoter, whereas PHLPP1 overexpression decreases both STAT1 Ser727 phosphorylation and transcriptional activity at the promoter. Second, both the IFNγ-induced phosphorylation of Ser727 and resulting increase in transcriptional activity at the GAS promoter are insensitive to OA, a phosphatase inhibitor that is ineffective towards PP2C family members but highly effective towards the abundant PP2A in cells. The insensitivity of STAT1 Ser727 phosphorylation to OA is consistent with PHLPP1 directly dephosphorylating this site in cells, a reaction it catalyzes *in vitro*. Furthermore, although PHLPP1 does suppress the signaling output of Akt (by dephosphorylating Ser473 (Gao et al., 2005)) and Erk (by reducing the steady-state levels of RTKs (Reyes et al., 2014)), its effect on STAT1 is unlikely to involve either of these targets because the activities of both kinases are sensitive to OA. Nor are the effects on Ser727 a result of PHLPP1 reducing PKC steady-state levels (Baffi et al., 2019), as the general PKC inhibitor Gö6983 did not alter GAS promoter activity (**Figure S4**). Third, genetic depletion of either PHLPP1 or STAT1 has opposing effects on transcriptional targets of STAT1: whereas KLA causes a larger increase in mRNA of *Cd69*, *Ifit2*, and *Gbp5* in BMDMs from *Phlpp1*$^{-/-}$ mice compared to WT mice, a reduction in these transcripts is observed upon STAT1 knockdown. Lastly, we have previously shown that PHLPP1 regulates transcription of genes and binds chromatin (Reyes et al., 2014). Cumulatively, these data are consistent with PHLPP1 being the major phosphatase to oppose the activating phosphorylation of STAT1 on Ser727, thereby limiting its transcriptional activity.

The interaction of PHLPP1 with STAT1, mediated by its NTE, affords fidelity and specificity in its dephosphorylation of the transcription factor. PHLPP1 binding to STAT1 is consistent with this multi-valent protein utilizing its protein-interaction domains to position it near its substrates, either via direct interaction or by binding protein scaffolds, such as PDZ domain proteins that coordinate Akt signaling (Li et al., 2011). Such coordination is essential for its dephosphorylation of relevant substrates, in part due to the low catalytic activity of the phosphatase (approximately 1 reaction per sec towards peptide substrates, an order of magnitude lower than that of the related phosphatase PP2Cα (Sierecki and Newton, 2014)). The importance of enzyme proximity to its substrate is best illustrated with Akt, where deletion of the last 3 amino acids of PHLPP1 to remove the PDZ ligand abolishes the ability of PHLPP1 to dephosphorylate Akt in cells (Gao et al., 2005). Thus, binding of PHLPP1 via its NTE to STAT1 affords an efficient mechanism to restrict its activity by directly opposing its phosphorylation in the nucleus (see **Figure 8**).

The regulation of STAT1 by PHLPP1 occurs in the nucleus, and we identify motifs in the phosphatase that control both the entry into (NLS) and exit from (NES) the nucleus. First, we identify a bipartite NLS in the NTE of PHLPP1 whose integrity is necessary for the phosphatase to regulate the transcriptional activity of STAT1. Second, we identify an NES in the segment between the LRR and PP2C domain that drives export out of the nucleus. Under the 'unstimulated' conditions of our immunocytochemistry, PHLPP1 localized primarily to the cytosol, suggesting masking of the NLS and exposure of the NES. Inputs that regulate the exposure of the NLS and NES are likely important regulators of PHLPP1 function.

Our transcriptomic data support a key role for PHLPP1 in the resolution of the inflammatory response specific to genes downstream of type II IFN signaling pathways. This

suggests the possibility that PHLPP1 can selectively discriminate between inflammatory promoters that are differentially regulated by distinct transcription factor families. Surprisingly, over 50% of the inflammatory genes that fail to properly resolve in the macrophages from *Phlpp1*$^{-/-}$ mice contain a consensus STAT-binding motif in their proximal promoters. Our studies have demonstrated a direct interaction between PHLPP1 and STAT1, thus it is highly likely that PHLPP1 is recruited to gene promoters through its association with STAT1. Elevated STAT1 occupancy and delayed dismissal kinetics of STAT1 from its target promoters in *Phlpp1*$^{-/-}$ macrophages indicate a major function of PHLPP1-dependent dephosphorylation in termination of STAT1 signaling and its dismissal from chromatin.

Germline mutations that impair STAT1 function, by reducing either Tyr701 phosphorylation (L706S) or DNA binding (Q463H and E320Q), increase the susceptibility of otherwise healthy patients to mycobacterial and viral infection (Chapgier et al., 2006; Dupuis et al., 2001). This increased susceptibility was proposed to arise because of reduced transcription of genes involved in bacterial and viral immunity from the GAS and ISRE promoters, respectively. Similarly, genetic ablation of *STAT1* on the background of a mouse that has enhanced TLR4 signaling (because of deletion of *gp130*, a key regulator of systemic inflammatory responses during LPS-mediated endotoxemia) provides protection against LPS-induced toxemic death compared to mice with normal STAT1 levels (Luu et al., 2014). Given the protective effect of PHLPP1 loss on both *E. coli*-induced sepsis and LPS-induced endotoxemia in mice, it is possible that PHLPP1 inhibitors could be explored as adjunctive therapies to antibiotics and supportive care of patients with Gram-negative sepsis, a leading cause of mortality in intensive care units.

EXPERIMENTAL PROCEDURES

Materials and Antibodies

OA (459616) was purchased from Millipore. Gö6983 (365251) and staurosporine (569397) were purchased from Calbiochem. Antibody against HA (11867425001) was purchased from Roche; antibodies against GFP (2555), STAT1 (9172), phosphorylated Ser727 on STAT1 (9177), phosphorylated Tyr701 on STAT1 (7649), phosphorylated Thr202/Tyr204 on Erk1/2 (9101), total Erk1/2 (9102), and phosphorylated Thr308 on Akt (9275) were purchased from Cell Signaling. Antibody against total Akt (126811) was obtained from AbCam. Antibodies against PHLPP1 were purchased from Cosmo (KIAA0606) and Proteintech (22789-1-AP); antibodies against FLAG (F3165), β-Actin (A2228), and α-tubulin (T6074) were purchased from Sigma-Aldrich. The pcDNA3 HA-tagged PHLPP1 and PHLPP2 constructs for mammalian cell expression were described previously (Brognard et al., 2007; Gao et al., 2008; Gao et al., 2005). Full-length PHLPP1 was cloned into pCMV 3xFLAG vector (Sigma-Aldrich, E4401). An NLS was cloned to the N-terminus of the PP2C domain of PHLPP1. A double mutant of NLS-PP2C at residues D1210A and D1413A was cloned by site-directed mutagenesis. The HA-tagged PHLPP1 N-terminal extension (PHLPP1 NTE), residues 1-512, was cloned into pcDNA3 vector (Invitrogen). The NLS1 and NLS2 mutations were cloned by site-directed mutagenesis into HA-PHLPP1 NTE. The NES from PKI (LALKLALDI) was cloned into the N-terminus of HA-PHLPP1 NTE. The PHLPP1 NES mutant was generated by site-directed mutagenesis.

Isolation and treatment of macrophages

Primary BMDM cells were isolated from male 6- to 8-week-old C57BL/6 mice (Charles River Laboratories). BMDMs were obtained by PBS flush of femurs and tibias (Weischenfeldt and Porse, 2008), red blood cells lysed, and remaining cells plated in RPMI 1640 supplemented with

403 20% fetal bovine serum (FBS, Gibco, cat. 12657-029), 30% L-cell conditioned medium, 100
404 U/ml penicillin, 100 µg/ml streptomycin, and 2 mM L-glutamine. Cells were seeded in non-
405 tissue culture treated Optilux Petri dishes (BD Biosciences), incubated at 37 °C in a 5% CO_2
406 atmosphere for 7 days, then treated with 100 ng/ml KLA (699500, Avanti Polar Lipids) for noted
407 times. Peritoneal macrophages were collected by flushing mouse peritoneal cavities with PBS
408 following 48 hours post peritoneal injection with 3 ml of thioglycolate (Ray and Dittel, 2010).

409 **Cell culture**

410 MEFs from WT or *Phlpp1*$^{-/-}$ mice stably expressing shp53 were a kind gift from Lloyd Trotman
411 (CSHL) and have been described previously (Chen et al., 2011); MEFs, HEK-293T, and HeLa
412 cells were grown in Dulbecco's modified Eagle medium (DMEM, 10-013-CV, Corning)
413 supplemented with 10% fetal bovine serum (S11150, Atlanta biologicals) and 1%
414 penicillin/streptomycin (15140-122, Gibco) at 37 °C in 5% (vol/vol) CO_2.

415 **mRNA isolation and qPCR analysis:**

416 RNA was purified using Direct-zol RNA Miniprep Kits (Zymo Research) from triplicate
417 experiments and quantified using a NanoDrop Spectrophotometer (ThermoFisher Scientific).
418 RNA was either reverse transcribed into cDNA for quantitative real-time PCR using gene-
419 specific primers or used for next-generation library preparation. For cDNA generation, one µg of
420 total mRNA was reverse transcribed using the SuperScript III Reverse Transcriptase
421 (ThermoFisher Scientific). The resulting cDNA (25 ng) was used to perform real-time PCR
422 using SYBR Green Master Mix (ThermoFisher Scientific) and 50 nM mix of forward and
423 reverse primers. The real-time PCR values for individual genes were normalized to the house
424 keeping gene, 36B4, using the ΔΔCT method (Livak and Schmittgen, 2001). The primer
425 sequences used in this study are:

*36B4*_qPCR_F	AATCTCCAGAGGCACCATTG
*36B4*_qPCR_R	CCGATCTGCAGACACACACT
*Cd69*_qPCR_F	CTATCCCTTGGGCTGTGTTAAT
*Cd69*_qPCR_R	ACATGGTGGTCAGATGATTCC
*Ifit2*_qPCR_F	GAGTTTGAGGACAGGGTGTTTA
*Ifit2*_qPCR_R	AGACCTCTGCAGTGCTTTAC
*Gbp5*_qPCR_F	GGAAGTGCTGCAGACCTATT
*Gbp5*_qPCR_R	GCTCTTTCTTGTTCCGCTTTAC

Next-generation sequence library preparation and analysis

Libraries were prepared from 2 biological replicates per condition. RNA-Seq libraries were prepared as previously described (Kaikkonen et al., 2013). Sequencing libraries were prepared using magnetic beads similar to described previously using barcoded adapters (NextFlex, Bioo Scientific) (Garber et al., 2012). Libraries were sequenced for 36 or 50 cycles on an Illumina Genome Analyzer II or HiSeq 2000, respectively, according to the manufacturer's instructions. mRNA-Seq results were trimmed to remove A-stretches originating from the library preparation. Each sequence tag returned by the Illumina Pipeline was aligned to the mm10 assembly using ELAND allowing up to 2 mismatches. Only tags that mapped uniquely to the genome were considered for further analysis. Peak finding, MOTIF discovery, and downstream analysis was performed using HOMER, a software suite created for analysis of high-throughput sequencing data (Heinz et al., 2010). Detailed instructions for analysis can be found at http://homer.ucsd.edu/homer/. Data visualization was performed using Microsoft Excel, JavaTreeGraph and software packages available in R.

RNA interference experiments

SMART siRNA pools for examined genes were purchased from Dharmacon (Control: D-001810-10-05, *Stat1*: L-058881). Thioglycollate-elicited peritoneal macrophages were transfected with 30 nM siRNA for 48 h using Deliver X (Affymetrix) according to the manufacturer's instructions prior to being stimulated with KLA for designated times.

Chromatin immunoprecipitation

ChIP assays were performed as described before (Stender et al., 2017). Cells were crosslinked with 2 mM disuccinimidyl glutarate for 30 min prior to 10 min treatment with 1% formaldehyde. The antibodies used in these studies were: STAT1 (sc-345, Santa Cruz Biotechnology). For the precipitations protein A Dynabeads (10003D, Invitrogen) were coated with antibody prior to pulldown and excess antibody was washed away. Pulldowns occurred while rotating for 16 h at 4 °C. Beads were then washed with TSE I (20 mMTris/HCl pH 7.4 at 20 °C, 150 mM NaCl, 0.1% SDS, 1% Triton X-100, 2 mM EDTA), twice with TSE III (10 mM Tris/HCl pH 7.4 at 20 °C, 250 mM LiCl, 1% IGEPAL CA-630, 0.7% Deoxycholate, 1 mM EDTA), and twice with TE followed by elution from the beads using elution buffer (0.1 M $NaHCO_3$, 1% SDS). Elutions were subsequently de-crosslinked overnight at 65 °C and DNA was purified using ChIP DNA Clean and Concentrator (Zymo Research) and DNA was used for qPCR. The primer sequences used in this study are:

*Cd69*_ChIP_F	TCCCTGCTGTCTGAAATGTG
*Cd69*_ChIP_R	GTGGAAGGATGTCTTCGATTCT
*Ifit2*_ChIP_F	GCATTGTGCAAGGAGAATTCTATG
*Ifit2*_ChIP_R	TTCCGGAATTGGGAGAGAGA
*Gbp5*_ChIP_F	TAAACAGCGCTTGAAACAATGA
*Gbp5*_ChIP_R	AGGCTTGAATGTCACTGAACTA

Luciferase assay

Cells were plated in a 96-well plate and transfected when approximately 80% confluent. Transfections of pRL-CMV encoding Renilla luciferase (Heinz et al., 2010), together with a firefly luciferase promoter-reporter construct containing eight GAS consensus sequences (Horvai et al., 1997), control vector, or the indicated PHLPP constructs, were performed using Lipofectamine 3000 reagent (Invitrogen, L3000) for MEFs or Fugene 6 reagent (Promega, E269A) for HEK-293T cells. Cells were treated with murine or human IFNγ (PeproTech, 315-05, 300-02, respectively) for the indicated times at 37 °C and activity was measured using the Dual-Glo Luciferase Assay System (Promega, E2940) in a Tecan Infinite M200 Pro multi-well plate reader. Promoter activity was corrected for the luciferase activity of the internal control plasmid, pRL-CMV, and Relative Response Ratios (RRR) were calculated.

Immunoprecipitation and western blot

DNA was transfected into HEK-293T cells using FuGene 6. Cells were collected 24 h post-transfection and then lysed in a buffer containing 50 mM Na_2HPO_4 (pH 7.5), 1 mM sodium pyrophosphate, 20 mM NaF, 2 mM EDTA, 2 mM EGTA, 1% SDS, 1 mM DTT, 1 µM microcystin, 20 µM benzamidine, 40 µg/ml leupeptin, and 1 mM PMSF and then were sonicated briefly. For co-immunoprecipitation, cells were lysed and the detergent-solubilized cell lysates were incubated with an anti-HA antibody (BioLegend, 901503) at 4 °C overnight. Samples were incubated with protein A/G PLUS-Agarose (Santa Cruz Cat sc-2003) for 1 h at 4 °C and washed three times in lysis buffer containing 0.3 M NaCl and 0.1% Triton X 100. Bound proteins and lysates were separated by SDS/PAGE gel and analyzed by western blot.

Immunofluorescence

HeLa cells were plated on glass coverslips and transfected using FuGene 6. 24 h after transfection, cells were fixed with 4% paraformaldehyde for 20 min at room temperature, followed by fixation with 100% methanol for 3 min at -20 °C. Cells were permeabilized and blocked in 0.3% Triton X 100 and 3% BSA for 30 min at room temperature, followed by three 5-min washes in PBS-T. Primary antibodies were diluted at the following dilutions: mouse anti-HA, 1:500; rabbit anti-α-tubulin (Cell Signaling, 2125), 1:200. Secondary antibodies were diluted at the following dilutions: Alexa647 anti-mouse (Life Technologies, A21235), 1:500; Alexa488 anti-rabbit (Life Technologies, A11034), 1:500. Coverslips were mounted onto slides with ProLong Diamond Antifade Mountant with DAPI (ThermoFisher, P36966). Images were acquired on a Zeiss Axiovert 200M microscope (Carl Zeiss Microimaging Inc.) using an iXon Ultra 888 EMCCD camera (ANDOR) controlled by MetaFluor software (Molecular Devices) and analyzed on ImageJ (NIH). The Nuclear to Cytoplasmic ratio was calculated as follows: the mean signal intensity was measured for a region of the nucleus and cytoplasm for each cell, and the mean signal intensity of the background was subtracted from these values. Then the Nuclear to Cytoplasmic ratio was calculated by dividing the background subtracted mean signal intensity for the nuclear signal by the background subtracted value for the cytoplasmic signal.

In vitro phosphatase assay

pCMV 3xFLAG PHLPP1 was transfected into HEK-293T cells plated in four 10 cm plates (approximately 9 x 10^6 cells per plate, 80% transfection efficiency) using Fugene 6. Cells were collected 48 h post-transfection and lysed in a buffer containing 20 mM Tris (pH 7.5), 150 mM NaCl, 1 mM EDTA, 1 mM EGTA, 1% Triton X 100, 2.5 mM sodium pyrophosphate, 1 mM Na_3VO_4, 1 mM DTT, 1 mM PMSF 1 µM microcystin, 20 µM benzamidine, and 40 µg/ml leupeptin. The detergent-solubilized cell lysates were incubated with anti-FLAG M2 affinity gel

(30 µl per plate, Sigma-Aldrich, A2220) for 1 h at 4 °C, washed four times in lysis buffer and the beads were resuspended in 40 µl 200 mM Tris, 4 mM DTT, 20 mM $MnCl_2$ for use in *in vitro* phosphatase assay. STAT1 (0.3 µM) (Biosource, PHF0011) was phosphorylated *in vitro* by incubation with recombinant human cdk1/cyclinB (0.2 µM) (Millipore, 14-450) at 30 °C for 90 min in the presence of 1 mM ATP, and 1 X PK buffer (NEB, B6022) containing 50 mM Tris, 10 mM $MgCl_2$, 0.1 mM EDTA, 2 mM DTT, 0.01% Brij, pH 7.5, and the reaction was quenched by addition of 144 µM CDK1 inhibitor RO3306 (Enzo, ALX-270-463). Phosphorylated STAT1 substrate was added to 1/4 volume of beads with bound PHLPP1 (or to lysis buffer control) and reactions were allowed to proceed for an additional 120 min at 30 °C. For the zero minute time point, beads were added after the 120 min incubation and all reactions were immediately quenched with 4xSB (sample buffer). Samples were analyzed by western blot.

Mouse infection and endotoxin challenge

Bacterial sepsis in mice was induced by injection of *E. coli* K1 strain RS218 and LPS endotoxemia was induced by injection of purified *E. coli* O111:B4 LPS (Sigma-Aldrich). The *E. coli* culture was grown overnight in Luria broth (LB) medium (Hardy Diagnostics) at 37°C with shaking. The bacterial culture was diluted 1:50 in fresh LB, grown to mid-log phase, washed twice with PBS and reconstituted in PBS to yield the appropriate inoculum. For survival experiments, 10 to 14-week-old female C57BL/6 WT and littermate control *Phlpp1*$^{-/-}$ mice were injected i.p. with 5 x 10^7 colony forming units (cfu) *E. coli* or 15 mg/kg LPS and mouse survival recorded for 10 days following injection. For measurement of serum IL-6, IL-10 and IL-1β levels, mice were injected with 10 mg/kg LPS, and at 4, 8, 12 and 24 h after injection, 80 µl of blood was collected by submandibular bleeding using a lancet into a serum separating blood collection tubes (BD) that were spun at 1500 × *g* for 10 min to separate serum. Serum cytokines

were quantified by specific ELISA (R&D) following the manufacturer's protocol. All protocols for mouse experiments were conducted in accordance with the institutional guidelines and were approved by the Institutional Animal Care and Usage Committee (IACUC) at the University of California, San Diego.

SUPPLEMENTAL INFORMATION

Supplemental Information includes Extended Experimental Procedures, four figures, and two tables and can be found with this article online.

AUTHOR CONTRIBUTIONS

K.C.-K., J.D.S., S.U., A.T.K., and G. L. performed the experiments. K.C.-K., J.D.S., and A.C.N. wrote the manuscript. K.C.-K., J.D.S., A.T.K, G. L., S.U., V.N., C.K.G. and A.C.N. conceived the project.

ACKNOWLEDGMENTS

We thank Maya Kunkel for advice and Mira Sastri, Gregory Fonseca, and Ali Syed for assistance with reagents and methodologies. This work was supported by NIH R35 GM122523 (A.C.N.), NIH GM067946 (A.C.N.), NIH HL125352 (V.N.), NIH DK091183 (C.K.G.) and DK063491 (C.K.G.). K.C.-K. was supported in part by NIH/NCI T32 CA009523 and A.T.K. was supported in part by the University of California San Diego Graduate Training Grant in Cellular and Molecular Pharmacology through the National Institutes of Health Institutional Training Grant T32 GM007752 from the NIGMS.

References

Alamuru, N.P., Behera, S., Butchar, J.P., Tridandapani, S., Kaimal Suraj, S., Babu, P.P., Hasnain, S.E., Ehtesham, N.Z., and Parsa, K.V. (2014). A novel immunomodulatory function of PHLPP1: inhibition of iNOS via attenuation of STAT1 ser727 phosphorylation in mouse macrophages. J Leukoc Biol *95*, 775-783.

Baffi, T.R., Van, A.N., Zhao, W., Mills, G.B., and Newton, A.C. (2019). Protein Kinase C Quality Control by Phosphatase PHLPP1 Unveils Loss-of-Function Mechanism in Cancer. Molecular cell.

Brognard, J., Sierecki, E., Gao, T., and Newton, A.C. (2007). PHLPP and a second isoform, PHLPP2, differentially attenuate the amplitude of Akt signaling by regulating distinct Akt isoforms. Molecular cell *25*, 917-931.

Chapgier, A., Boisson-Dupuis, S., Jouanguy, E., Vogt, G., Feinberg, J., Prochnicka-Chalufour, A., Casrouge, A., Yang, K., Soudais, C., Fieschi, C., *et al.* (2006). Novel STAT1 alleles in otherwise healthy patients with mycobacterial disease. PLoS genetics *2*, e131.

Chen, M., Pratt, C.P., Zeeman, M.E., Schultz, N., Taylor, B.S., O'Neill, A., Castillo-Martin, M., Nowak, D.G., Naguib, A., Grace, D.M., *et al.* (2011). Identification of PHLPP1 as a tumor suppressor reveals the role of feedback activation in PTEN-mutant prostate cancer progression. Cancer cell *20*, 173-186.

Chen, M.J., Dixon, J.E., and Manning, G. (2017). Genomics and evolution of protein phosphatases. Science signaling *10*.

Coussens, L.M., and Werb, Z. (2002). Inflammation and cancer. Nature *420*, 860-867.

Darnell, J.E., Jr. (1997). STATs and gene regulation. Science *277*, 1630-1635.

Darnell, J.E., Jr., Kerr, I.M., and Stark, G.R. (1994). Jak-STAT pathways and transcriptional activation in response to IFNs and other extracellular signaling proteins. Science *264*, 1415-1421.

Dawson, M.A., and Kouzarides, T. (2012). Cancer epigenetics: from mechanism to therapy. Cell *150*, 12-27.

Dupuis, S., Dargemont, C., Fieschi, C., Thomassin, N., Rosenzweig, S., Harris, J., Holland, S.M., Schreiber, R.D., and Casanova, J.L. (2001). Impairment of mycobacterial but not viral immunity by a germline human STAT1 mutation. Science *293*, 300-303.

Flavahan, W.A., Gaskell, E., and Bernstein, B.E. (2017). Epigenetic plasticity and the hallmarks of cancer. Science *357*.

Fu, S.C., Imai, K., and Horton, P. (2011). Prediction of leucine-rich nuclear export signal containing proteins with NESsential. Nucleic acids research *39*, e111.

Fullerton, J.N., and Gilroy, D.W. (2016). Resolution of inflammation: a new therapeutic frontier. Nat Rev Drug Discov *15*, 551-567.

Gao, T., Brognard, J., and Newton, A.C. (2008). The phosphatase PHLPP controls the cellular levels of protein kinase C. The Journal of biological chemistry *283*, 6300-6311.

Gao, T., Furnari, F., and Newton, A.C. (2005). PHLPP: a phosphatase that directly dephosphorylates Akt, promotes apoptosis, and suppresses tumor growth. Molecular cell *18*, 13-24.

Garber, M., Yosef, N., Goren, A., Raychowdhury, R., Thielke, A., Guttman, M., Robinson, J., Minie, B., Chevrier, N., Itzhaki, Z., *et al.* (2012). A high-throughput chromatin immunoprecipitation approach reveals principles of dynamic gene regulation in mammals. Molecular cell *47*, 810-822.

Grivennikov, S.I., Greten, F.R., and Karin, M. (2010). Immunity, inflammation, and cancer. Cell *140*, 883-899.

Grzechnik, A.T., and Newton, A.C. (2016). PHLPPing through history: a decade in the life of PHLPP phosphatases. Biochemical Society transactions *44*, 1675-1682.

Hein, M.Y., Hubner, N.C., Poser, I., Cox, J., Nagaraj, N., Toyoda, Y., Gak, I.A., Weisswange, I., Mansfeld, J., Buchholz, F., *et al.* (2015). A human interactome in three quantitative dimensions organized by stoichiometries and abundances. Cell *163*, 712-723.

Heinz, S., Benner, C., Spann, N., Bertolino, E., Lin, Y.C., Laslo, P., Cheng, J.X., Murre, C., Singh, H., and Glass, C.K. (2010). Simple combinations of lineage-determining transcription factors prime cis-regulatory elements required for macrophage and B cell identities. Molecular cell *38*, 576-589.

598 Horvai, A.E., Xu, L., Korzus, E., Brard, G., Kalafus, D., Mullen, T.M., Rose, D.W., Rosenfeld, M.G., and
599 Glass, C.K. (1997). Nuclear integration of JAK/STAT and Ras/AP-1 signaling by CBP and p300.
600 Proceedings of the National Academy of Sciences of the United States of America *94*, 1074-1079.
601 Jernberg, E., Bergh, A., and Wikstrom, P. (2017). Clinical relevance of androgen receptor alterations in
602 prostate cancer. Endocr Connect *6*, R146-R161.
603 Kaikkonen, M.U., Spann, N.J., Heinz, S., Romanoski, C.E., Allison, K.A., Stender, J.D., Chun, H.B.,
604 Tough, D.F., Prinjha, R.K., Benner, C., *et al.* (2013). Remodeling of the enhancer landscape during
605 macrophage activation is coupled to enhancer transcription. Molecular cell *51*, 310-325.
606 Kalkat, M., De Melo, J., Hickman, K.A., Lourenco, C., Redel, C., Resetca, D., Tamachi, A., Tu, W.B.,
607 and Penn, L.Z. (2017). MYC Deregulation in Primary Human Cancers. Genes (Basel) *8*.
608 Karin, M., Lawrence, T., and Nizet, V. (2006). Innate immunity gone awry: linking microbial infections
609 to chronic inflammation and cancer. Cell *124*, 823-835.
610 Li, X., Yang, H., Liu, J., Schmidt, M.D., and Gao, T. (2011). Scribble-mediated membrane targeting of
611 PHLPP1 is required for its negative regulation of Akt. EMBO Rep *12*, 818-824.
612 Lin, J.R., and Hu, J. (2013). SeqNLS: nuclear localization signal prediction based on frequent pattern
613 mining and linear motif scoring. PloS one *8*, e76864.
614 Liu, J., Weiss, H.L., Rychahou, P., Jackson, L.N., Evers, B.M., and Gao, T. (2009). Loss of PHLPP
615 expression in colon cancer: role in proliferation and tumorigenesis. Oncogene *28*, 994-1004.
616 Livak, K.J., and Schmittgen, T.D. (2001). Analysis of relative gene expression data using real-time
617 quantitative PCR and the 2(-Delta Delta C(T)) Method. Methods *25*, 402-408.
618 Luu, K., Greenhill, C.J., Majoros, A., Decker, T., Jenkins, B.J., and Mansell, A. (2014). STAT1 plays a
619 role in TLR signal transduction and inflammatory responses. Immunol Cell Biol *92*, 761-769.
620 O'Neill, L.A., Golenbock, D., and Bowie, A.G. (2013). The history of Toll-like receptors - redefining
621 innate immunity. Nature reviews. Immunology *13*, 453-460.
622 O'Shea, J.J., and Murray, P.J. (2008). Cytokine signaling modules in inflammatory responses. Immunity
623 *28*, 477-487.
624 Ohmori, Y., and Hamilton, T.A. (2001). Requirement for STAT1 in LPS-induced gene expression in
625 macrophages. J Leukoc Biol *69*, 598-604.
626 Oishi, Y., Spann, N.J., Link, V.M., Muse, E.D., Strid, T., Edillor, C., Kolar, M.J., Matsuzaka, T.,
627 Hayakawa, S., Tao, J., *et al.* (2017). SREBP1 Contributes to Resolution of Pro-inflammatory TLR4
628 Signaling by Reprogramming Fatty Acid Metabolism. Cell metabolism *25*, 412-427.
629 Patterson, S.J., Han, J.M., Garcia, R., Assi, K., Gao, T., O'Neill, A., Newton, A.C., and Levings, M.K.
630 (2011). Cutting edge: PHLPP regulates the development, function, and molecular signaling pathways of
631 regulatory T cells. J Immunol *186*, 5533-5537.
632 Pejerrey, S.M., Dustin, D., Kim, J.A., Gu, G., Rechoum, Y., and Fuqua, S.A.W. (2018). The Impact of
633 ESR1 Mutations on the Treatment of Metastatic Breast Cancer. Horm Cancer.
634 Platanias, L.C. (2005). Mechanisms of type-I- and type-II-interferon-mediated signalling. Nat Rev
635 Immunol *5*, 375-386.
636 Ray, A., and Dittel, B.N. (2010). Isolation of mouse peritoneal cavity cells. J Vis Exp.
637 Reyes, G., Niederst, M., Cohen-Katsenelson, K., Stender, J.D., Kunkel, M.T., Chen, M., Brognard, J.,
638 Sierecki, E., Gao, T., Nowak, D.G., *et al.* (2014). Pleckstrin homology domain leucine-rich repeat protein
639 phosphatases set the amplitude of receptor tyrosine kinase output. Proceedings of the National Academy
640 of Sciences of the United States of America *111*, E3957-3965.
641 Rossetto, D., Avvakumov, N., and Cote, J. (2012). Histone phosphorylation: a chromatin modification
642 involved in diverse nuclear events. Epigenetics : official journal of the DNA Methylation Society *7*, 1098-
643 1108.
644 Sabapathy, K., and Lane, D.P. (2018). Therapeutic targeting of p53: all mutants are equal, but some
645 mutants are more equal than others. Nat Rev Clin Oncol *15*, 13-30.
646 Sadzak, I., Schiff, M., Gattermeier, I., Glinitzer, R., Sauer, I., Saalmuller, A., Yang, E., Schaljo, B., and
647 Kovarik, P. (2008). Recruitment of Stat1 to chromatin is required for interferon-induced serine

phosphorylation of Stat1 transactivation domain. Proceedings of the National Academy of Sciences of the United States of America *105*, 8944-8949.

Sierecki, E., and Newton, A.C. (2014). Biochemical characterization of the phosphatase domain of the tumor suppressor PH domain leucine-rich repeat protein phosphatase. Biochemistry *53*, 3971-3981.

Stark, G.R., and Darnell, J.E., Jr. (2012). The JAK-STAT pathway at twenty. Immunity *36*, 503-514.

Stender, J.D., Nwachukwu, J.C., Kastrati, I., Kim, Y., Strid, T., Yakir, M., Srinivasan, S., Nowak, J., Izard, T., Rangarajan, E.S., *et al.* (2017). Structural and Molecular Mechanisms of Cytokine-Mediated Endocrine Resistance in Human Breast Cancer Cells. Molecular cell *65*, 1122-1135 e1125.

Weischenfeldt, J., and Porse, B. (2008). Bone Marrow-Derived Macrophages (BMM): Isolation and Applications. CSH Protoc *2008*, pdb prot5080.

Wen, W., Meinkoth, J.L., Tsien, R.Y., and Taylor, S.S. (1995a). Identification of a signal for rapid export of proteins from the nucleus. Cell *82*, 463-473.

Wen, Z., Zhong, Z., and Darnell, J.E., Jr. (1995b). Maximal activation of transcription by Stat1 and Stat3 requires both tyrosine and serine phosphorylation. Cell *82*, 241-250.

Whitmarsh, A.J., and Davis, R.J. (2000). Regulation of transcription factor function by phosphorylation. Cellular and molecular life sciences : CMLS *57*, 1172-1183.

Wynn, T.A., and Vannella, K.M. (2016). Macrophages in Tissue Repair, Regeneration, and Fibrosis. Immunity *44*, 450-462.

FIGURE LEGENDS

Figure 1

PHLPP1 knock-out mice are protected against sepsis-induced death. (**A**) Survival curve of WT and *Phlpp1*$^{-/-}$ mice i.p. infected with 1x10^{7} cfu of *E. coli*. Values are expressed as percent survival of 15 mice for each genotype. ** $p < 0.01$ by log-rank test. (**B**) Survival curve of WT and *Phlpp1*$^{-/-}$ mice i.p. injected with 15 mg/kg LPS. Values are expressed as percent survival of 16 mice for each genotype. * $p < 0.04$ by log-rank test. (**C-E**) ELISA showing IL-6 (**C**), IL-1β (**D**) and IL-10 (**E**) levels in serum at the indicated times after i.p. injection of 10 mg/kg LPS. Data represent mean ± SEM. Statistics analyzed by Student's *t*-test *$p < 0.05$, **$p < 0.01$.

Figure 2

Loss of PHLPP1 modulates the expression of inflammatory genes in macrophages. (**A**) Heat map for mRNA-Seq expression of the 1,654 mRNA transcripts regulated greater than two-fold with a FDR < 0.05 in BMDMs isolated from WT or *Phlpp1*$^{-/-}$ animals treated with 100 ng/ml KLA for 1, 6 or 24 h. Data represent the $\log_2$ difference between the mRNA expression in *Phlpp1*$^{-/-}$ macrophages compared to wild-type macrophages. (**B**) Gene ontology analysis for the 199 elevated (red arrow) or 144 decreased (blue arrow) transcripts in *Phlpp1*$^{-/-}$ macrophages compared to wild-type macrophages. (**C**) *De novo* motif analysis using HOMER (Hypergeometric Optimization of Motif EnRichment) for the 199 promoters corresponding to the genes elevated in the *Phlpp1*$^{-/-}$ macrophages. (**D**) Pie graph showing the percentage of promoters of elevated genes that contain STAT or IRF binding motifs. (**E-G**) Normalized mRNA-Seq values for (**E**) *Cd69* (**F**) *Ifit2* and (**G**) *Gbp5* mRNA in BMDMs isolated from WT or *Phlpp1*$^{-/-}$ animals treated with 100 ng/ml KLA for 0, 1, 6, or 24 h. RPKM – Reads Per Kilobase Million.

690 Values are expressed as mean ± SEM. *p < 0.05 (Student's *t*-test) compared to WT cells. See
691 also Tables S1 and S2.

692 **Figure 3**

693 PHLPP1 controls STAT1 genomic recruitment and STAT1-dependent gene expression. (**A-C**)
694 Quantitative PCR analysis for (**A**) *Cd69* (**B**) *Ifit2* and (**C**) *Gbp5* mRNA isolated from
695 thioglycollate-elicited peritoneal macrophages treated with control siRNA (siCtl) or siRNA
696 specifically targeting *Stat1* (si*Stat1*) and subsequently treated with vehicle or 100 ng/ml KLA for
697 6 or 24 h. Values are expressed as mean ± SEM from replicate experiments. *p < 0.05 (Student's
698 *t*-test) compared to siCtl treated cells. (**D-F**) Quantitative PCR analysis of ChIPs for STAT1 at
699 the (**D**) *Cd69* (**E**) *Ifit2* and (**F**) *Gbp5* promoter in BMDMs isolated from WT or *Phlpp1*$^{-/-}$ animals
700 and treated with 100 ng/ml KLA for 0, 1, 6 or 24 h. Values are expressed as mean ± SEM. *p <
701 0.05 (Student's *t*-test) compared to WT cells.

702 **Figure 4**

703 PHLPP1 regulates STAT1 phosphorylation on Ser727. (**A**) Western blot analysis of primary
704 BMDM from WT or *Phlpp1*$^{-/-}$ mice treated with 100 ng/ml KLA for the indicated times and
705 probed with the indicated antibodies. (**B**) Ratio of pSTAT1 (S727):total STAT1, pSTAT1
706 (Y701):total STAT1 or phosphoERK (T202/Y204):total ERK normalized to the highest value;
707 data represent the mean ± SEM of five independent experiments as in (A). ** p < 0.01 (Student's
708 *t*-test) compared to WT cells. (**C**) Western blot analysis of an *in vitro* phosphatase assay of
709 purified and phosphorylated STAT1 and immunoprecipitated FLAG-PHLPP1, incubated for 0
710 and 120 min at 30 °C (on the left). On the right, quantification of pSTAT1 (S727) divided by
711 total STAT1 and normalized to 0 time point. Values are expressed as mean ± SEM of three

712 independent experiments. ** $p < 0.01$ (Student's *t*-test). (**D**) Western blot analysis of HEK-293T
713 cells over-expressing vector control (Vector) or HA-tagged PHLPP1 and treated with 10 ng/ml
714 IFNγ for 0, 1, 6, or 24 h. (**E**) Graphs represent the quantification of three independent
715 experiments as presented in (D). Values are expressed as mean relative units of pSTAT1 (S727)
716 or (Y701) divided by β-Actin and normalized to vector 0 h ± SEM. * $p < 0.05$ (Student's *t*-test)
717 compared to vector control expressing cells. See also Figure S1.
718

719 **Figure 5**

720 STAT1 Ser727 phosphorylation and transcriptional activity are insensitive to okadaic acid. (**A**)
721 Western blot analysis of primary BMDMs from WT or *Phlpp1*$^{-/-}$ mice treated with 100 ng/ml
722 KLA for 0 or 30 min followed by treatment with 1 μM OA or DMSO control for an additional
723 15 min. and probed with the indicated antibodies; pAkt antibody recognizes phosphorylated
724 Thr308 (**B**) Graph represents the quantification of three independent experiments as presented in
725 (A). Values are expressed as the mean ± SEM of the ratio of pSTAT1 (S727) to total STAT1
726 normalized to the highest value; * $p<0.05$, ** $p<0.01$ and n.s.- non-significant (Student's *t*-test).

727 **Figure 6**

728 PHLPP1 suppresses STAT1 transcriptional activity by a mechanism that depends on its catalytic
729 activity and an NLS in its N-Terminal Extension (**A**) Luciferase reporter assay in WT (+/+) and
730 *Phlpp1*$^{-/-}$ (-/-) MEFs over-expressing GAS luciferase reporter and treated with 10 ng/ml IFNγ for
731 0, 1, 6, or 24 h in combination with 1 μM OA or DMSO control treatment for 15 minutes. Values
732 are expressed as mean of relative light units (RLU) ± SEM of three independent experiments. *p
733 < 0.05 (Student's *t*-test). See also Figure S1. (**B**) Schematic of HA-tagged PHLPP1 constructs
734 used in this study: the PP2C domain of PHLPP1 (PP2C), nuclear targeted PP2C with NLS (NLS-

PP2C), NLS-PP2C with active site residues Asp1210 and Asp1413 residues mutated to Ala (NLS-PP2C DDAA), and full-length PHLPP1 (PHLPP1). (**C**) Luciferase reporter assay in HEK-293T cells over-expressing GAS luciferase reporter in combination with either vector control (vector, black) or the constructs described in (B) and treated with 10 ng/ml IFNγ for 0, 1, 6, or 24 h. Values are expressed as mean RLU ± SEM of four independent experiments. All data points at 24 h were significant against each other except for vector to PP2C, vector to NLS-PP2C DDAA, P1 to NLS-PP2C, and PP2C to NLS-PP2C DDAA. * $p < 0.05$, ** $p < 0.01$(Student's *t*-test). (**D**) Schematic showing position and sequence of bipartite NLS in the NTE, and NLS mutants used in this study. (**E**) HeLa cells over-expressing the constructs used in Figure 6D were stained for HA (green), α-Tubulin (red), and DAPI (blue). Scale bar indicates 15 µm. (**F**) The Nuclear to Cytoplasmic ratio was calculated for each construct (300 cells per construct) and values are expressed as mean ± SEM. All data points were significant against each other except for NLS1 to NLS2, and NLS2 to NLS1/2. ** $p < 0.01$, n.s. – non-significant (Student's *t*-test).(**G**) Luciferase reporter assay in HEK-293T cells over-expressing a GAS luciferase reporter in combination with either vector control (vector, black) or the constructs described in (D) however in the context of a full-length PHLPP1 and treated with 10 ng/ml IFNγ for 0, 1, 6, or 24 h. Values are expressed as mean RLU ± SEM of eight independent experiments. *$p < 0.05$, **$p < 0.01$, n.s. - non-significant (Student's *t*-test).

Figure 7

(**A**) Luciferase reporter assay in HEK-293T cells over-expressing GAS luciferase reporter in combination with either vector control (Vector, black), PHLPP1 NTE (NTE, green), PHLPP1ΔNTE (blue), or PHLPP1 (red) and treated with 10 ng/ml IFNγ for 0, 1, 6, or 24 h. Values are expressed as mean of RLU ± SEM of five independent experiments. All data points at

24 h were significant against each other except for vector to PHLPP1ΔNTE, and PHLPP1ΔNTE to PHLPP1. * $p < 0.05$, ** $p < 0.01$, *** $p < 0.001$ (Student's *t*-test). (**B**) Western blot analysis of detergent-solublized lysate of HEK-293T cells transfected with vector control (Vector), HA-tagged NTE of PHLPP1, PHLPP1 with the NTE deleted (P1ΔNTE) or full-length PHLPP1 (HA-P1) and immunoprecipitated (IP) using HA antibody; blots were probed for co-IP of STAT1 tag using GFP antibody. (**C**) Quantification of GFP-STAT1 IP divided by HA IP and normalized to HA-NTE IP. Values are expressed as mean ± SEM of three independent experiments. *** $p < 0.001$, **** $p < 0.0001$ (Student's *t*-test).

Figure 8

Proposed model for PHLPP1-dependent suppression of STAT1 activity. Binding of IFNγ to IFN receptors results in their dimerization and phosphorylation, promoting the recruitment of JAK, which phosphorylates STAT1 on Tyr701 by JAK. This promotes the dimerization of STAT1 and its translocation into the nucleus where it binds the GAS promoter to allow the transcription of inflammatory response genes. Activity of STAT1 is enhanced by phosphorylation on Ser727. However, PHLPP1, which binds STAT1 via its N-terminal extension, tunes the activity of STAT1 by directly dephosphorylating this site to keep activity finely controlled. Loss of PHLPP1 results in poor resolution of inflammatory response.

Table S1. Related to Figure 2.

List of 199 KLA-induced genes that are elevated in *Phlpp1*$^{-/-}$ BMDMs compared to WT cells.

Table S2. Related to Figure 2.

List of 144 KLA-induced genes that are reduced in *Phlpp1*$^{-/-}$ BMDMs compared to WT cells.

Figure S1 related to Figure 6.

STAT1 phosphorylation and transcriptional activity are insensitive to okadaic acid. Western blot analysis of extracts used in the luciferase reporter assay in WT (+/+) and *Phlpp1*$^{-/-}$ (-/-) MEFs over-expressing GAS luciferase reporter and treated with 10 ng/ml IFNγ for 0, 1, 6, or 24 h in combination with 1 μM OA or DMSO control treatment for 15 minutes. Phosphorylation of the PP2A target site on Akt (Thr308) was increased upon OA treatment.

Figure S2 related to Figure 6.

The phosphatase activity of PHLPP1 is important for the regulation of STAT1 activity. (**A**) HeLa cells over-expressing the HA-tagged constructs used in Figure 6B were stained for HA (green), α-Tubulin (red), and DAPI (blue). Scale bar indicates 15 μm. (**B**) The Nuclear to Cytoplasmic ratio was calculated for each construct and values are expressed as mean ± SEM of: 169 cells for P1, 101 cells for PP2C, 100 cells for NLS-PP2C, and 101 cells for NLS-PP2C DDAA.

Figure S3. Related to Figure 6.

PHLPP1 has an NES. (**A**) Schematic showing position of NES (residues 1121-1134) immediately following the last LRR. (**B**) HeLa cells over-expressing PHLPP1, the NTE from WT PHLPP1 (NTE-WT) or the NTE-WT in which the PHLPP1 NES was fused to the N-terminus (^{PHLPP1}NES-NTE) were stained for HA (green), α-Tubulin (red), and DAPI (blue). Scale bar indicates 15 μm.

Figure S4. Related to Discussion.

801 Luciferase reporter assay in HEK-293T cells over-expressing GAS luciferase reporter and
802 treated with 10 ng/ml IFNγ for 0, 1, 6, or 24 h followed by 250 nM Gö6983 for 10 min, 1 µM
803 staurosporine for 30 min, or DMSO control. Values are expressed as mean of RLU ± SEM of
804 three independent experiments.
805

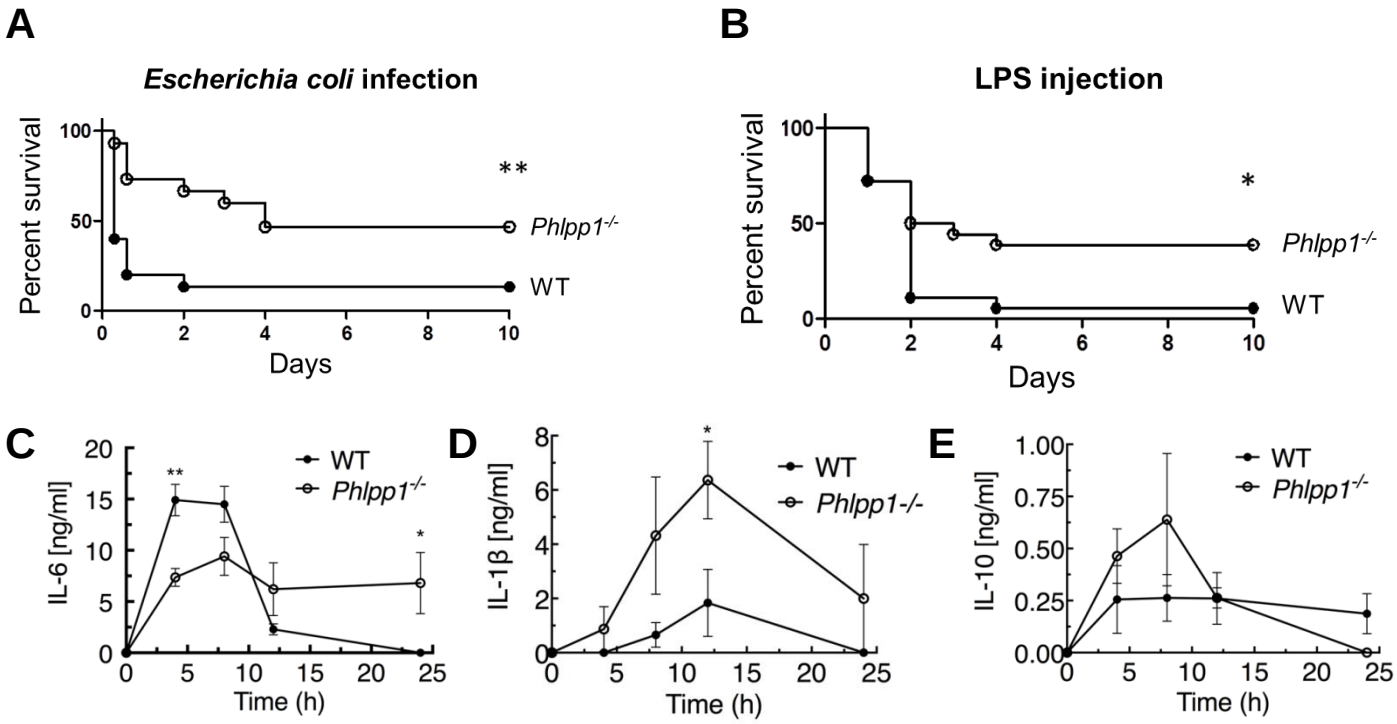
A
Escherichia coli infection
Percent survival
100
50
0
0
2
4
6
8
10
Days
**
Phlpp1-/-
WT
B
LPS injection
Percent survival
100
50
0
0
2
4
6
8
10
Days
*
Phlpp1-/-
WT
C
IL-6 [ng/ml]
20
15
10
5
0
0
5
10
15
20
25
Time (h)
**
*
WT
Phlpp1-/-
D
IL-1β [ng/ml]
8
6
4
2
0
0
5
10
15
20
25
Time (h)
*
WT
Phlpp1-/-
E
IL-10 [ng/ml]
1.00
0.75
0.50
0.25
0.00
0
5
10
15
20
25
Time (h)
WT
Phlpp1-/-

Figure 1

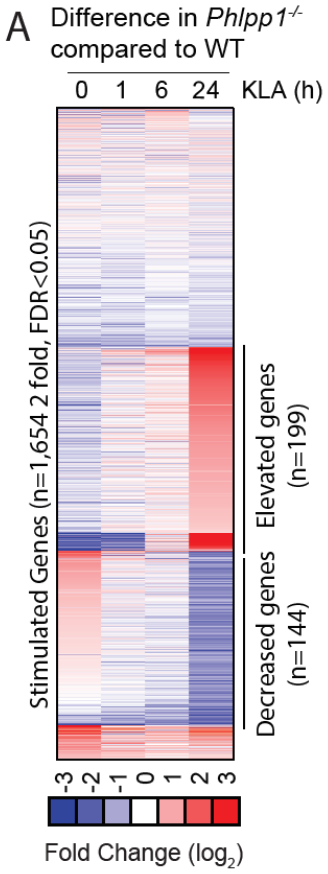

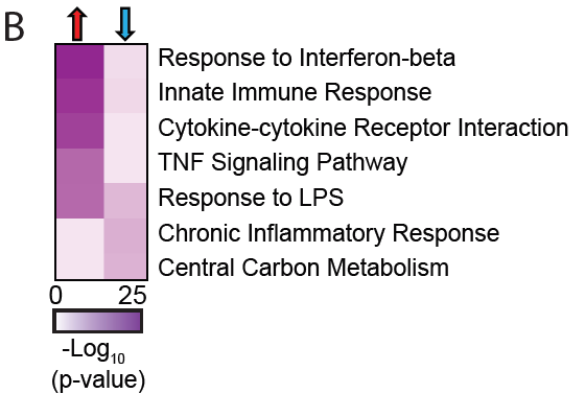

C

Enriched motifs in promoters of elevated genes

Motif	p-value	Factor	% Promoters with motif
	p<1E-18	STAT	46%
	p<1E-9	IRF	51%

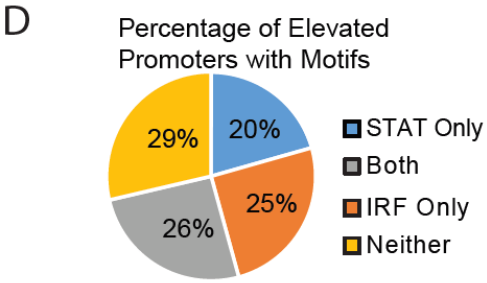

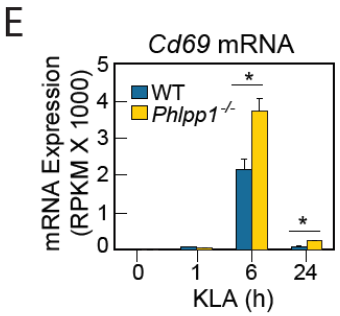

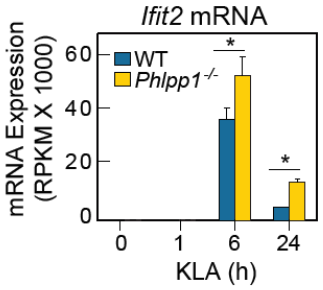

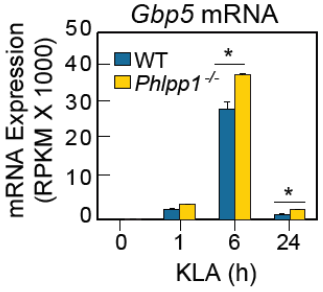

Figure 2

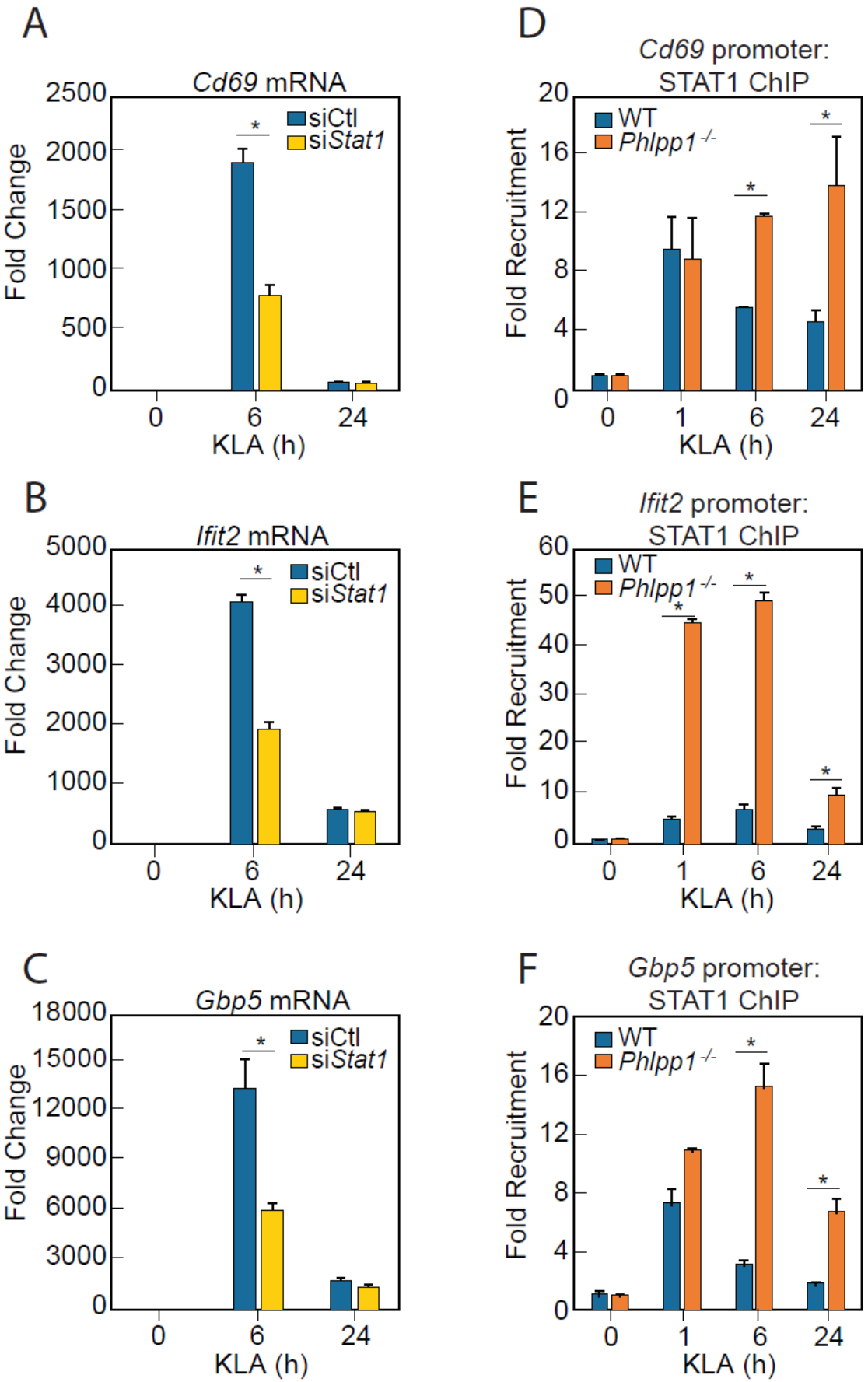
A
Cd69 mRNA
siCtl
siStat1
Fold Change
2500
2000
1500
1000
500
0
0
6
24
KLA (h)
*
B
Ifit2 mRNA
siCtl
siStat1
Fold Change
5000
4000
3000
2000
1000
0
0
6
24
KLA (h)
*
C
Gbp5 mRNA
siCtl
siStat1
Fold Change
18000
15000
12000
9000
6000
3000
0
0
6
24
KLA (h)
*
D
Cd69 promoter:
STAT1 ChIP
WT
Phlpp1 -/-
Fold Recruitment
20
16
12
8
4
0
0
1
6
24
KLA (h)
*
E
Ifit2 promoter:
STAT1 ChIP
WT
Phlpp1 -/-
Fold Recruitment
60
50
40
30
20
10
0
0
1
6
24
KLA (h)
*
F
Gbp5 promoter:
STAT1 ChIP
WT
Phlpp1 -/-
Fold Recruitment
20
16
12
8
4
0
0
1
6
24
KLA (h)
*

Figure 3

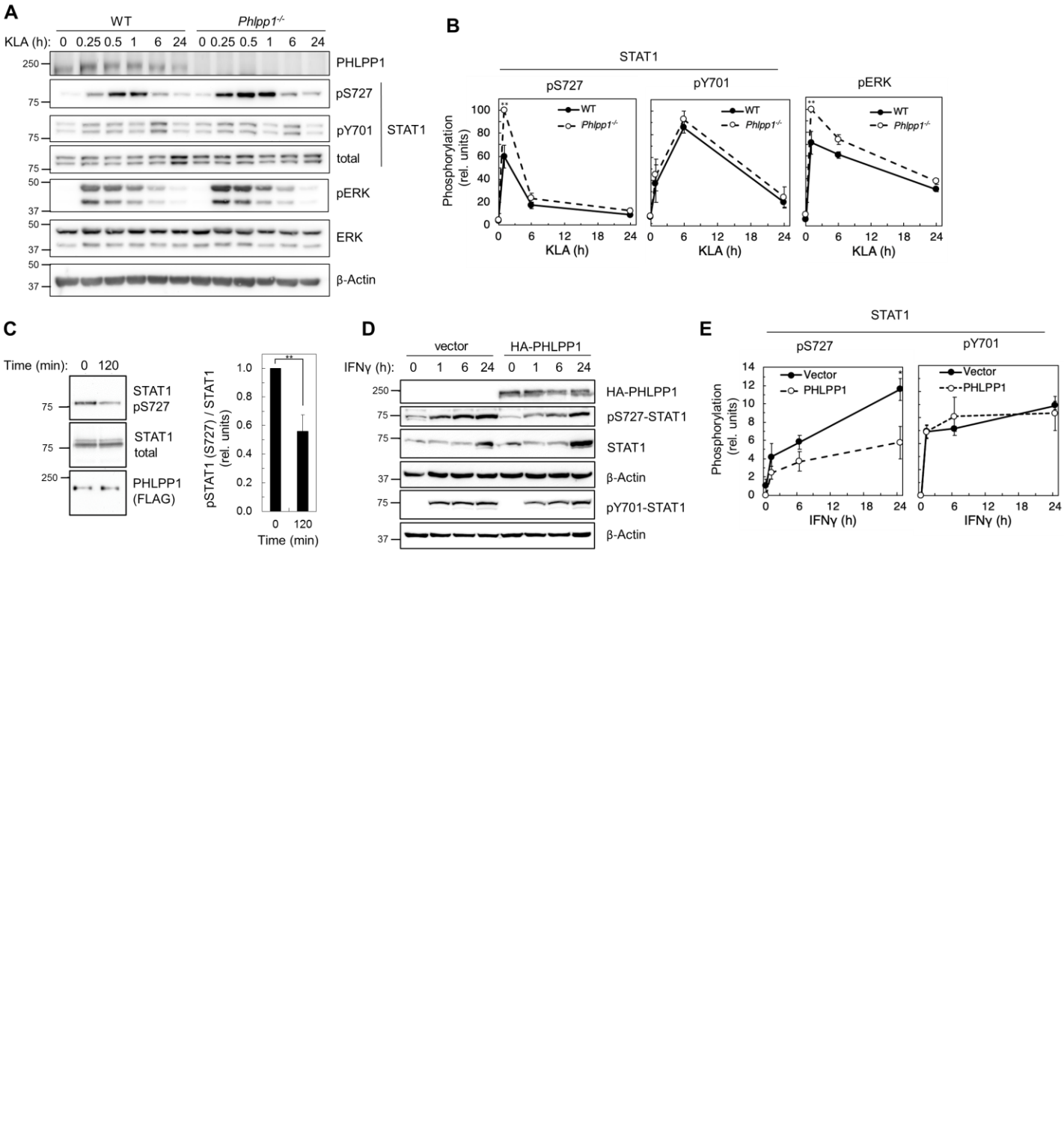
A
WT
Phlpp1-/-
KLA (h): 0 0.25 0.5 1 6 24 0 0.25 0.5 1 6 24
PHLPP1
pS727
pY701
total
STAT1
pERK
ERK
β-Actin
B
STAT1
pS727
pY701
pERK
Phosphorylation (rel. units)
WT
Phlpp1-/-
KLA (h)
C
Time (min): 0 120
STAT1 pS727
STAT1 total
PHLPP1 (FLAG)
pSTAT1 (S727) / STAT1 (rel. units)
Time (min)
D
vector
HA-PHLPP1
IFNγ (h): 0 1 6 24 0 1 6 24
HA-PHLPP1
pS727-STAT1
STAT1
β-Actin
pY701-STAT1
β-Actin
E
STAT1
pS727
pY701
Phosphorylation (rel. units)
Vector
PHLPP1
IFNγ (h)

Figure 4

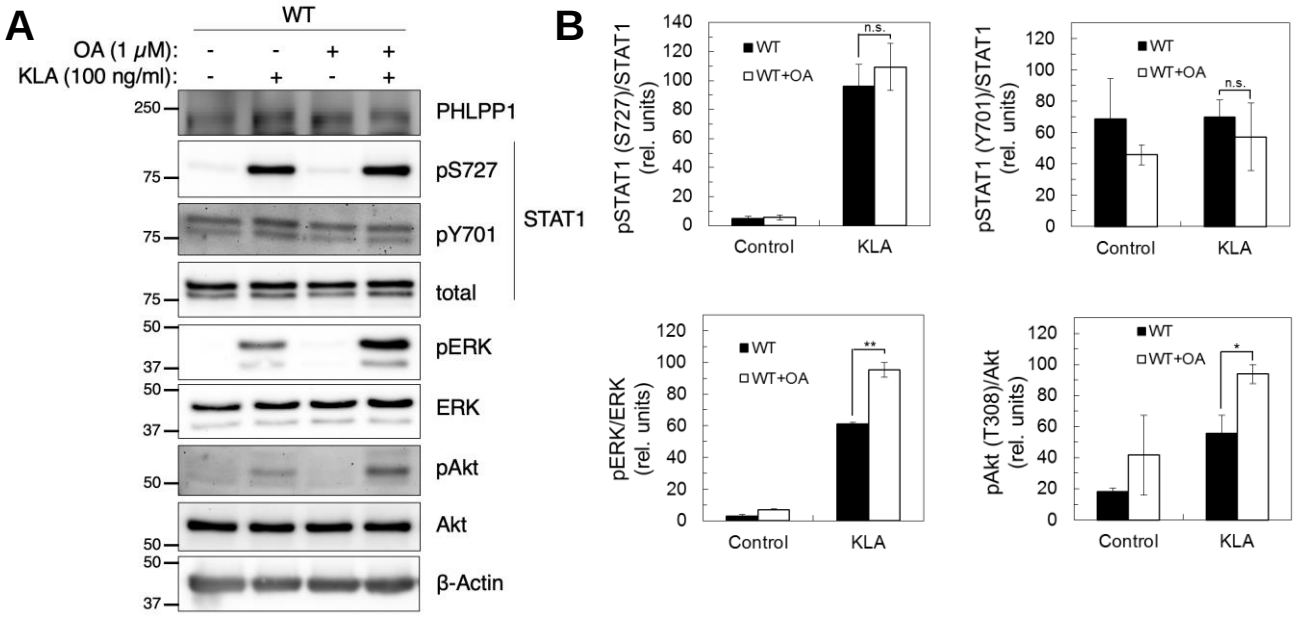
A
WT
OA (1 μM): - - + +
KLA (100 ng/ml): - + - +
250
PHLPP1
75
pS727
75
pY701
STAT1
75
total
50
37
pERK
50
37
ERK
50
pAkt
50
Akt
50
37
β-Actin
B
pSTAT1 (S727)/STAT1 (rel. units)
WT
WT+OA
n.s.
Control
KLA
pSTAT1 (Y701)/STAT1 (rel. units)
n.s.
pERK/ERK (rel. units)
**
pAkt (T308)/Akt (rel. units)
*

Figure 5

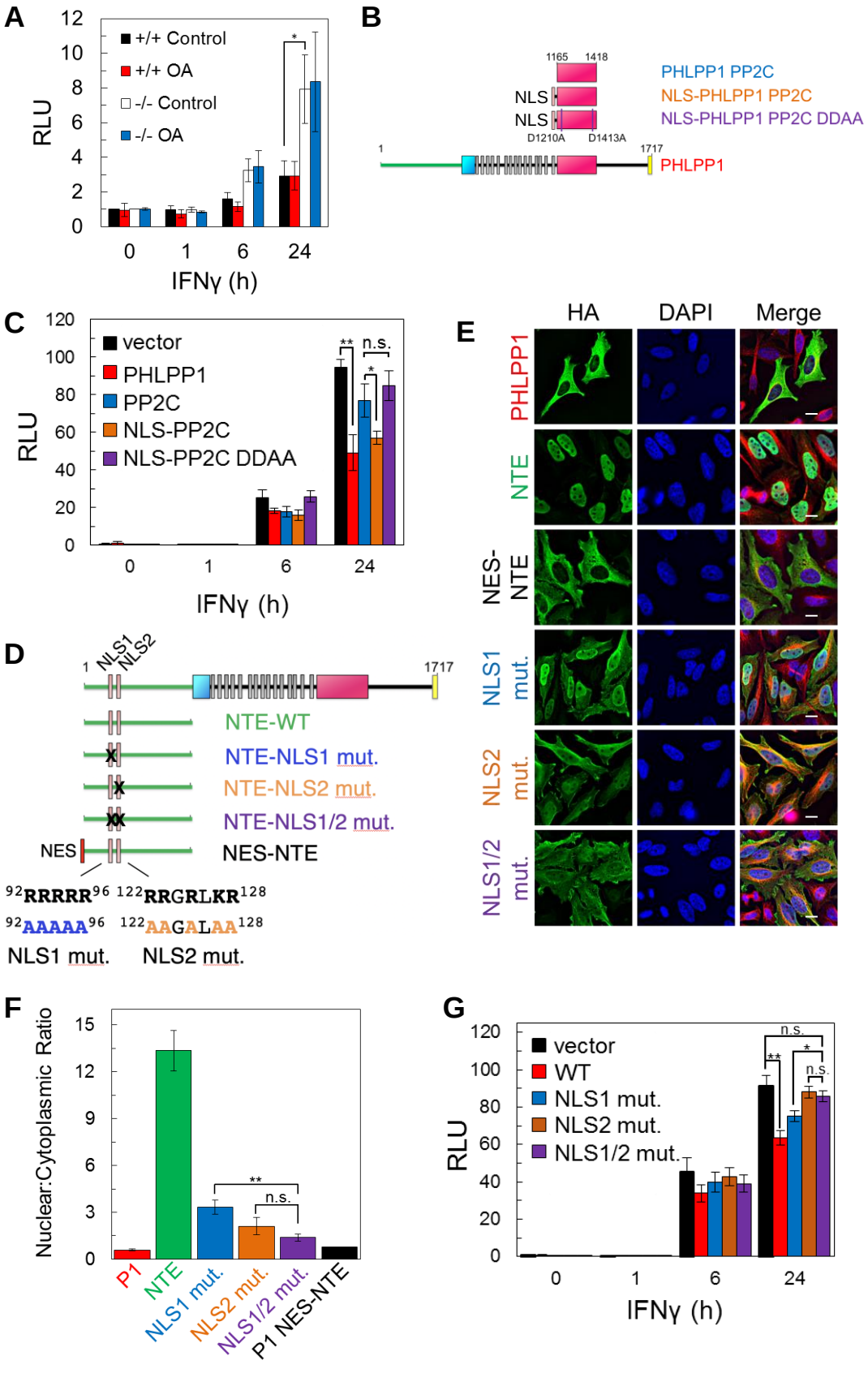
A
RLU
+/+ Control
+/+ OA
-/- Control
-/- OA
IFNγ (h)
B
PHLPP1 PP2C
NLS-PHLPP1 PP2C
NLS-PHLPP1 PP2C DDAA
NLS
D1210A
D1413A
PHLPP1
C
vector
PHLPP1
PP2C
NLS-PP2C
NLS-PP2C DDAA
n.s.
IFNγ (h)
D
NLS1
NLS2
NTE-WT
NTE-NLS1 mut.
NTE-NLS2 mut.
NTE-NLS1/2 mut.
NES
NES-NTE
92RRRRR96 122RRGRLKR128
92AAAAA96 122AAGALAA128
NLS1 mut.
NLS2 mut.
E
HA
DAPI
Merge
PHLPP1
NTE
NES-NTE
NLS1 mut.
NLS2 mut.
NLS1/2 mut.
F
Nuclear:Cytoplasmic Ratio
P1
NTE
NLS1 mut.
NLS2 mut.
NLS1/2 mut.
P1 NES-NTE
n.s.
G
vector
WT
NLS1 mut.
NLS2 mut.
NLS1/2 mut.
RLU
IFNγ (h)

Figure 6

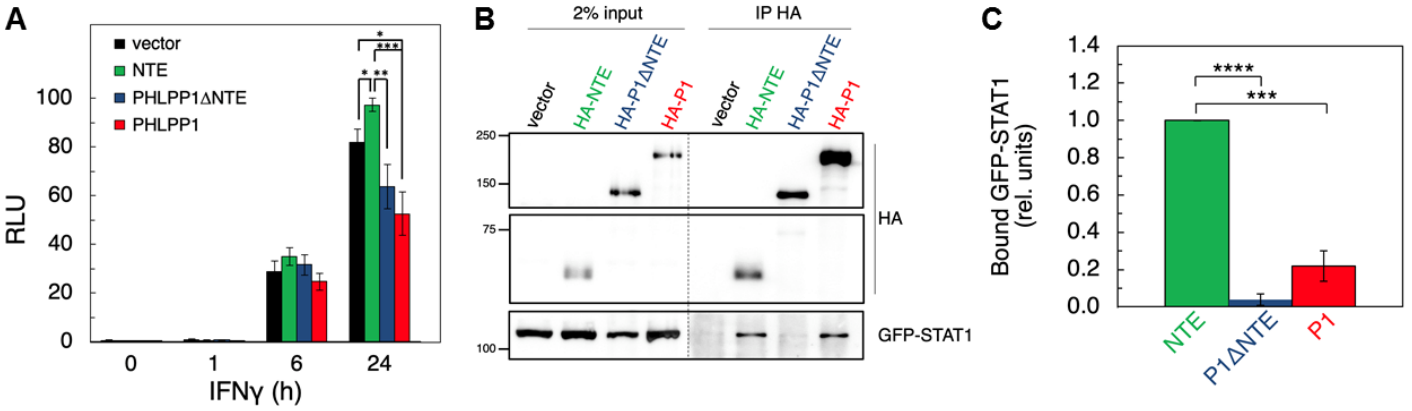
A
vector
NTE
PHLPP1ΔNTE
PHLPP1
RLU
IFNγ (h)
B
2% input
IP HA
vector
HA-NTE
HA-P1ΔNTE
HA-P1
HA
GFP-STAT1
C
Bound GFP-STAT1 (rel. units)
NTE
P1ΔNTE
P1

Figure 7

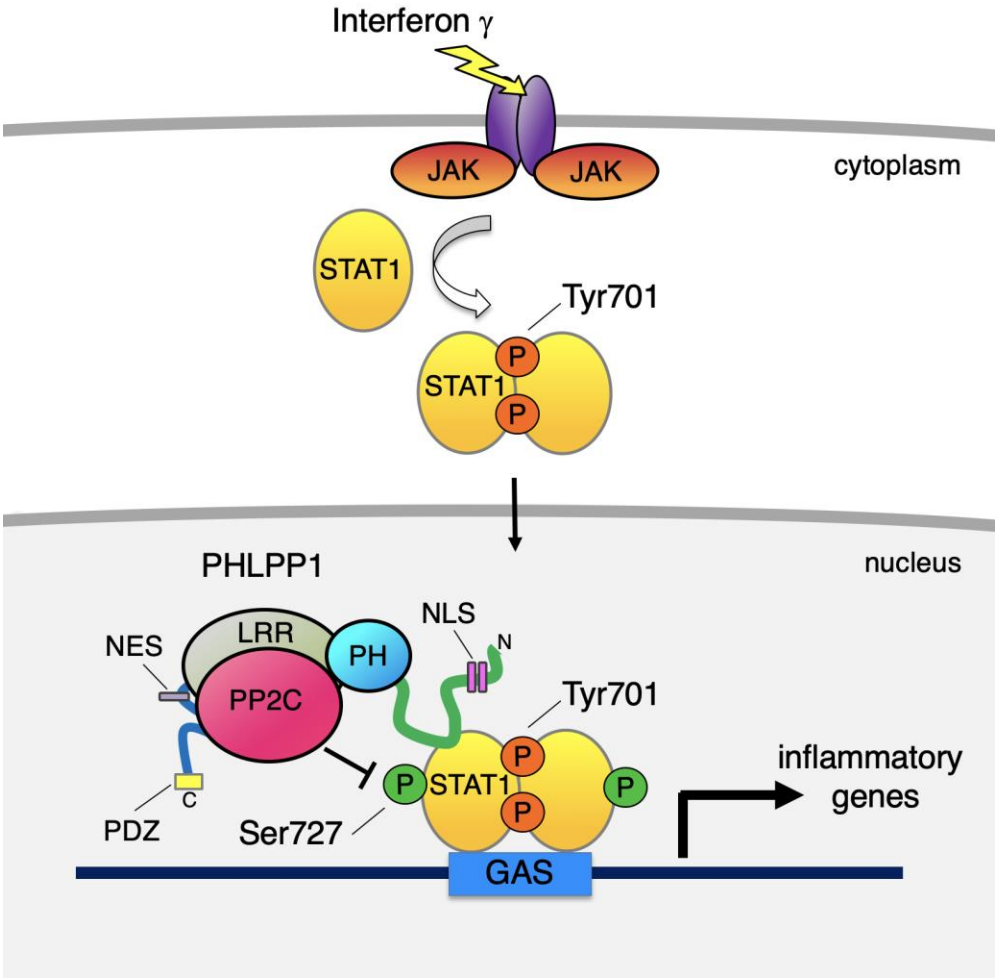
Interferon γ
JAK
JAK
cytoplasm
STAT1
Tyr701
P
STAT1
P
PHLPP1
nucleus
NES
LRR
PH
NLS
N
PP2C
Tyr701
P
P
STAT1
P
P
inflammatory
genes
C
PDZ
Ser727
GAS

Figure 8

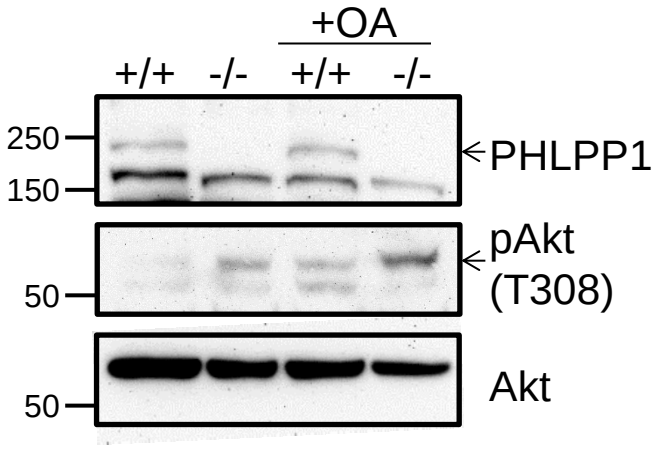

Figure S1

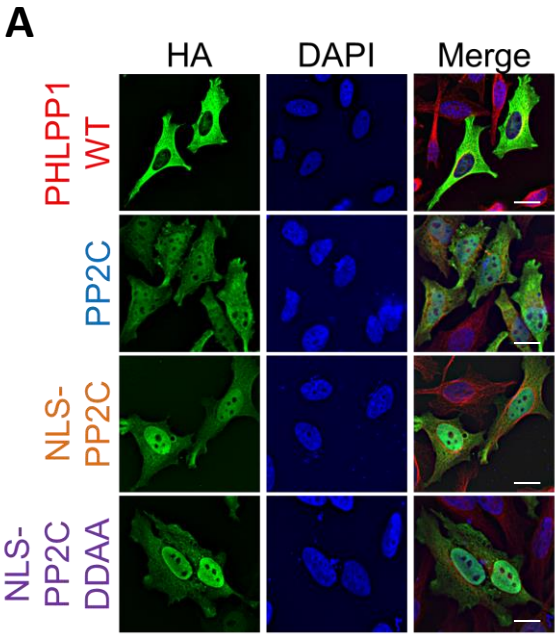
A
HA
DAPI
Merge
PHLPP1 WT
PP2C
NLS-PP2C
NLS-PP2C DDAA

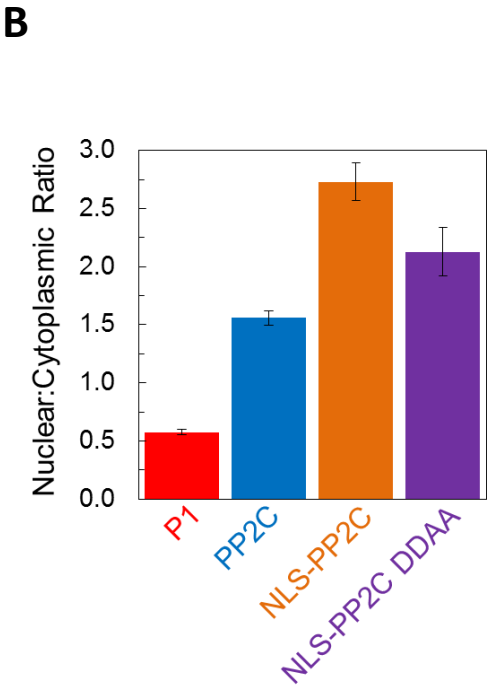
B
Nuclear:Cytoplasmic Ratio
3.0
2.5
2.0
1.5
1.0
0.5
0.0
P1
PP2C
NLS-PP2C
NLS-PP2C DDAA

Figure S2

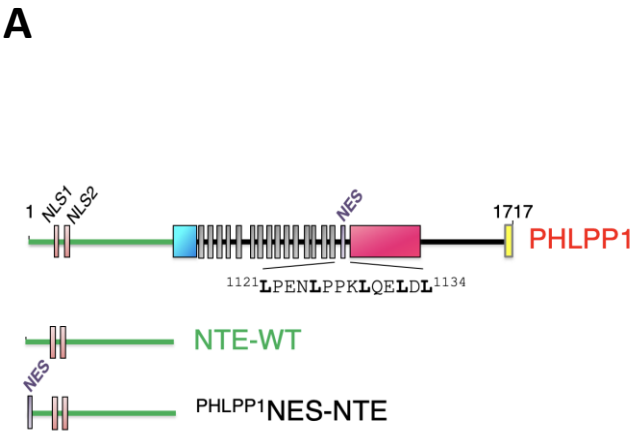
A
1
NLS1
NLS2
NES
1717
PHLPP1
1121LPENLPPKLQELDL1134
NTE-WT
NES
PHLPP1NES-NTE

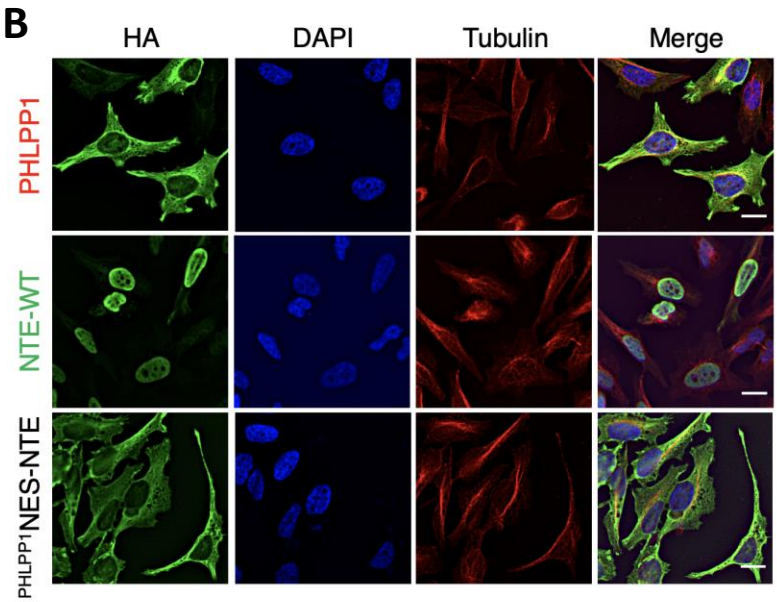
B
HA
DAPI
Tubulin
Merge
PHLPP1
NTE-WT
PHLPP1NES-NTE

Figure S3

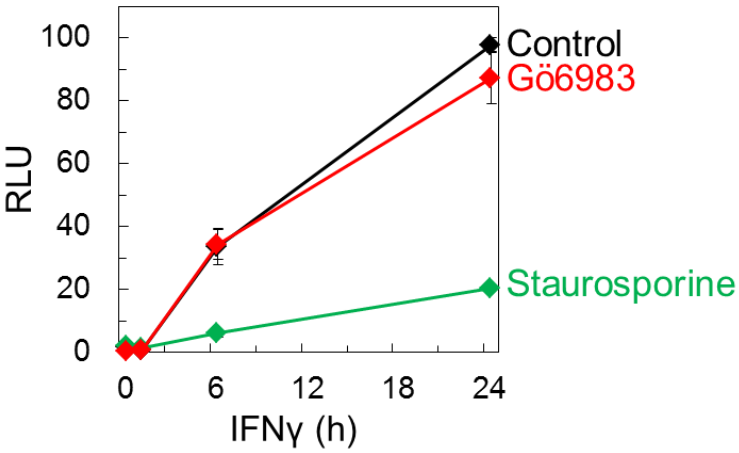
100
80
60
40
20
0
RLU
0
6
12
18
24
IFNγ (h)
Control
Gö6983
Staurosporine

Figure S4